

Convection and AGN feedback in clusters of galaxies

Benjamin D. G. Chandran

benjamin.chandran@unh.edu

Space Science Center and Department of Physics, University of New Hampshire

Yann Rasera

yann.rasera@unh.edu

Space Science Center and Department of Physics, University of New Hampshire

ABSTRACT

A number of studies have shown that the convective stability criterion for the intracluster medium (ICM) is very different from the Schwarzschild criterion due to the effects of anisotropic thermal conduction and cosmic rays. Building on these studies, we develop a model of the ICM in which a central active galactic nucleus (AGN) accretes hot intracluster plasma at the Bondi rate and produces cosmic rays that cause the ICM to become convectively unstable. The resulting convection heats the intracluster plasma and regulates its temperature and density profiles. By adjusting a single parameter in the model (the size of the cosmic-ray acceleration region), we are able to achieve a good match to the observed density and temperature profiles in a sample of eight clusters. Our results suggest that convection is an important process in cluster cores. An interesting feature of our solutions is that the cooling rate is more sharply peaked about the cluster center than is the convective heating rate. As a result, in several of the clusters in our sample, a compact cooling flow arises in the central region with a size r_{cf} that is typically a few kpc. The cooling flow matches onto a Bondi flow at smaller radii. The mass accretion rate in the Bondi flow is equal to, and controlled by, the rate at which mass flows in through the cooling flow. Our solutions suggest that the AGN regulates the mass accretion rate in these clusters by controlling r_{cf} : if the AGN power rises above the equilibrium level, r_{cf} decreases, the mass accretion rate drops, and the AGN power drops back down to the equilibrium level.

Subject headings: cooling flows — galaxies:clusters:general — galaxies:active — convection — magnetic fields — turbulence

1. Introduction

Active galactic nuclei (AGNs) have enormous mechanical and radiative luminosities. If an AGN’s power can be transferred to the surrounding interstellar and intergalactic media, the resulting heating can have a large effect on the ambient plasma. There has recently been great interest in this process of “AGN feedback,” its role in galaxy formation, and the possibility that AGN feedback solves the over-cooling problem (Suginohara & Ostriker 1998, Lewis et al 2000, Tornatore et al 2003, Nagai & Kravtsov 2004) and cooling-flow problem for clusters of galaxies (Böhringer et al 20001; David et al 2001; Tamura et al 2001; Molendi & Pizzolato 2001; Blanton, Sarazin, & McNamara 2003; Peterson et al 2001, 2003).

One of the main unsolved problems for AGN feedback is to understand how AGN power is transferred to the diffuse ambient plasma. A number of mechanisms have been investigated, including Compton heating (Binney & Tabor 1995; Ciotti & Ostriker 1997, 2001; Ciotti, Ostriker, & Pellegrini 2004, Sazonov et al 2005), shocks (Tabor & Binney 1993, Binney & Tabor 1995), magnetohydrodynamic (MHD) wave-mediated plasma heating by cosmic rays (Böhringer & Morfill 1988; Rosner & Tucker 1989; Loewenstein, Zweibel, & Begelman 1991), and cosmic-ray bubbles produced by the central AGN (Churazov et al 2001, 2002; Reynolds 2002; Brüggen 2003; Reynolds et al 2005), which can heat intracluster plasma by generating turbulence (Loewenstein & Fabian 1990, Churazov et al 2004) and sound waves (Fabian et al 2003; Ruszkowski, Brüggen, & Begelman 2004a,b) and by doing $p dV$ work (Begelman 2001, 2002; Ruszkowski & Begelman 2002; Hoeft & Brüggen 2004). Despite this substantial progress, it is still not clear how AGN feedback controls the density and temperature profiles of the ambient plasma in a way that is both self-regulating and consistent with observations.

In this paper, we focus on clusters of galaxies and explore the hypothesis that central AGNs heat and regulate the intracluster plasma by causing the intracluster medium to become convectively unstable, a scenario that was investigated in two earlier studies [Chandran (2004) (hereafter Paper I) and Chandran (2005) (hereafter Paper II)]. At first glance, this hypothesis seems obviously incorrect, since observations show that the specific entropy s in intracluster plasmas increases with radius r . However, several recent studies have shown that the Schwarzschild criterion ($ds/dr > 0$) does not apply to low-density, magnetized plasmas such as those found in clusters, in which the charged-particle gyroradii are much less than the Coulomb mean free path. In such plasmas, heat and charged particles diffuse primarily along magnetic field lines, and only weakly across the magnetic field. This anisotropy turns out to have a profound effect on convective stability, as shown analytically by Balbus (2000, 2001) and numerically by Parrish & Stone (2005, 2007). These authors considered a stratified plasma in which the gravitational acceleration is in the $-z$ direction and the equilibrium magnetic field is in the xy -plane and showed that the convective stability criterion is $dT/dz > 0$, not $ds/dz > 0$, where T is the temperature. When cosmic rays are present, the con-

vective stability criterion becomes $nk_B dT/dz + dp_{\text{cr}}/dz > 0$, as shown analytically by Chandran & Dennis (2006) and numerically by Rasera & Chandran (2007). Here, n and p_{cr} are the thermal-plasma number density and cosmic-ray pressure, respectively. In galaxy clusters, the gravitational acceleration is in the $-r$ direction, and the convective stability criterion is

$$nk_B \frac{dT}{dr} + \frac{dp_{\text{cr}}}{dr} > 0. \quad (1)$$

(Paper II and appendix B provide a more extensive discussion.) Although $dT/dr > 0$ in cluster cores, equation (1) shows that cosmic rays produced by an AGN at the center of a cluster can lead to convective instability, since centrally produced cosmic rays satisfy $dp_{\text{cr}}/dr < 0$.

In this paper, we construct a spherically symmetric, steady-state model of convective intra-cluster plasmas using mixing-length theory, and compare this model to observations. We assume that a central supermassive black hole accretes hot intracluster plasma at the Bondi rate, and converts a small fraction of the accreted rest-mass energy into cosmic rays that are accelerated by shocks within some distance r_{source} of the center of the cluster. The resulting cosmic-ray pressure gradient leads to convection, which in turn heats the thermal plasma in the cluster core by advecting internal energy inwards and allowing the cosmic rays to do pdV work on the thermal plasma. The model also includes thermal conduction, cosmic-ray diffusion, and radiative cooling. The model involves much less emission from plasma at temperatures below one-third of the cluster’s average temperature than the cooling flow model (Fabian 1994), and thus offers a possible solution to the cooling-flow problem.

We compare the density and temperature profiles predicted by the model to the profiles inferred from X-ray observations of eight clusters. We adjust a single parameter, the size r_{source} of the cosmic-ray acceleration region, to optimize the fit. The model solutions match the observations well, with the exception of the density with the central $\simeq 50$ kpc of Sersic 159-03, which is underestimated by the model. We suggest a possible explanation for this discrepancy in section 3. We also find that the cosmic-ray luminosities of the AGN in our sample are strongly correlated with the observationally inferred mechanical luminosities of these AGN. Our results suggest that AGN-driven convection is an important process in cluster cores.

An attractive feature of this model and other models based on AGN feedback and Bondi accretion is that they are self-regulating. One argument for why Bondi accretion is self-regulating was advanced by Nulsen (2004) and Böhringer et al (2004), who noted that the Bondi accretion rate is a monotonically decreasing function of the specific entropy near the center of the cluster. Thus, if the central plasma becomes too cool, the Bondi accretion rate rises, the AGN feedback heating increases, and the specific entropy of the central plasma rises back to its equilibrium value. In this paper, we offer an additional explanation for how AGN heating on large scales ($\gtrsim 5$ kpc) can regulate the mass accretion rate onto the central black hole. In our solutions, we find that the

radiative cooling rate is more sharply peaked about the center of a cluster than is the convective heating rate. As a result, in several of the clusters in our sample, the central region becomes a cooling flow. The radius of this cooling flow, r_{cf} , is typically a few kpc in our solutions. At smaller radii, the flow makes a transition from a cooling flow to a Bondi flow. However, as in the work of Quataert & Narayan (2000), the mass accretion rate of the inner Bondi flow is controlled by the surrounding cooling flow. In our model, which has no mass dropout, the mass accretion rate is approximately the plasma mass interior to r_{cf} divided by the cooling time at r_{cf} . The AGN then regulates the mass accretion rate by controlling r_{cf} : if the AGN power rises above the equilibrium level, the size of the central cooling flow decreases, the mass accretion rate drops, and the AGN power then drops back down to the equilibrium level.

This paper extends the previous models of paper I and paper II in several ways. In contrast to paper I, the present paper takes into account the role of anisotropic thermal conduction and cosmic-ray diffusion, which strongly modify the convective stability criterion. In contrast to paper II, we take the cosmic-ray acceleration to occur within a relatively small fraction of the total volume at any given radius, which allows for localized pockets of excess cosmic-ray pressure that tend to rise buoyantly. We also take into account the nonzero average radial velocity, and compare the model to a larger sample of clusters.

The rest of this paper is organized as follows. We present the basic equations of the model in section 2. In section 3, we compare our model calculations to observations. In section 4 we consider the radial profiles of the different heating rates and the factors that determine whether AGN feedback or thermal conduction is the dominant heat source at $r \lesssim 100$ kpc. In section 5 we discuss the central cooling flows that arise in our model solutions for several of the clusters in our sample. We also comment in section 5 on the viability of the Bondi accretion model for the AGN at the centers of clusters. We summarize our results in section 6. We present results on the radial profiles of the turbulent velocity and cosmic-ray pressure in appendix A. In appendix B we present a systematic derivation of the two-fluid mixing-length theory that we employ in our model.

2. Model equations

We describe the intracluster medium using a standard set of two-fluid equations for cosmic rays and thermal plasma (Drury & Volk 1981, Jones & Kang 1990), modified to include thermal conduction, viscous dissipation, and radiative cooling:

$$\frac{d\rho}{dt} = -\rho \nabla \cdot \mathbf{v}, \quad (2)$$

$$\rho \frac{dv}{dt} = -\nabla(p + p_{\text{cr}}) - \rho \nabla \Phi - \nabla \cdot \Pi_{\text{visc}}, \quad (3)$$

$$\frac{dp}{dt} = -\gamma p \nabla \cdot \mathbf{v} + (\gamma - 1)[H_{\text{visc}} + \nabla \cdot (\kappa \cdot \nabla T) - R], \quad (4)$$

and

$$\frac{dp_{\text{cr}}}{dt} = -\gamma_{\text{cr}} p_{\text{cr}} \nabla \cdot \mathbf{v} + \nabla \cdot (\mathbf{D} \cdot \nabla p_{\text{cr}}) + (\gamma_{\text{cr}} - 1) \dot{E}_{\text{source}}, \quad (5)$$

where

$$\frac{d}{dt} \equiv \frac{\partial}{\partial t} + \mathbf{v} \cdot \nabla, \quad (6)$$

ρ is the plasma density, \mathbf{v} is the bulk velocity of the two-fluid mixture, p and p_{cr} are the plasma and cosmic-ray pressures, T is the plasma temperature, Φ is the gravitational potential, Π_{visc} is the viscous stress tensor, γ and γ_{cr} are the plasma and cosmic-ray adiabatic indices (which are treated as constants), H_{visc} is the rate of viscous heating, κ is the thermal conductivity tensor, R is the radiative cooling rate, \dot{E}_{source} is the rate of injection of cosmic-ray energy per unit volume by the central radio source, and \mathbf{D} is an effective momentum-averaged cosmic-ray diffusion tensor. For the calculations presented in section 3, we set $\gamma = 5/3$ and $\gamma_{\text{cr}} = 4/3$. We ignore radiative cooling of cosmic rays, which is reasonable if protons make the dominant contribution to the cosmic-ray pressure. We also neglect Coulomb interactions between cosmic rays and thermal plasma, as well as wave-mediated heating of the thermal plasma by cosmic rays. As discussed below, we take into account the effects of the magnetic field on κ and \mathbf{D} , but we neglect the Lorentz force and resistive dissipation. In the following subsections, we describe the approximations we use to solve the above equations.

2.1. Mixing length theory

To account for convection, we write each fluid quantity as an average value plus a turbulent fluctuation:

$$\mathbf{v} = \langle \mathbf{v} \rangle + \delta \mathbf{v}, \quad (7)$$

$$p = \langle p \rangle + \delta p, \quad (8)$$

etc, where $\langle \dots \rangle$ denotes an average over the turbulent fluctuations. We take the averaged quantities to be spherically symmetric and independent of time, and we treat the fluctuating quantities as small. To obtain equations for the average cluster properties, we average equations (2) through (5). We evaluate the averages $\langle \rho \mathbf{v} \rangle$, $\langle \mathbf{v} p \rangle$, and $\langle \mathbf{v} p_{\text{cr}} \rangle$ in equations (2), (4), and (5) using a two-fluid mixing-length theory that we describe in appendix B. The essential idea behind this theory is that the amplitudes of the turbulent fluctuations increase as the average plasma and cosmic-ray profiles move past the point of marginal stability towards increasing degrees of convective instability. As this happens, the magnitudes of the internal energy flux $\langle \mathbf{v} p \rangle / (\gamma - 1)$ and the cosmic-ray energy flux $\langle \mathbf{v} p_{\text{cr}} \rangle / (\gamma_{\text{cr}} - 1)$ increase, which in turn affects the density, temperature, and cosmic-ray-pressure

profiles. The two-fluid mixing length theory provides an approximate way of determining the resulting profiles as well as the r -dependent turbulent velocity in a self-consistent way. A key parameter of the model is the mixing length l , which characterizes the length scale of the convective turbulence. We set

$$l = 0.4r. \quad (9)$$

2.2. Hydrostatic equilibrium

We assume that the convection is subsonic and confine our model to $r \geq 0.2$ kpc, so that the average radial velocity remains subsonic throughout our solutions. As a result, we can to a reasonable approximation drop the inertial terms in the average of equation (3). The viscous term in equation (3) is important primarily for dissipating small-scale velocity fluctuations and can also be neglected in the average of equation (3). The average of equation (3) then reduces to

$$\frac{d}{dr} \langle p_{\text{tot}} \rangle = -\langle \rho \rangle \frac{d\Phi}{dr}, \quad (10)$$

where

$$p_{\text{tot}} = p + p_{\text{cr}}. \quad (11)$$

2.3. Gravitational potential

We take the gravitational potential to be the sum of four components,

$$\Phi = \Phi_c + \Phi_s + \Phi_{\text{bh}} + \Phi_p, \quad (12)$$

where Φ_c is the contribution from the the cluster's dark matter, Φ_s is the contribution from the stars in the brightest cluster galaxy (BCG), Φ_{bh} is the contribution from the black hole at $r = 0$, and Φ_p is the contribution from the intracluster plasma. We take the cluster dark matter to have an NFW density profile (Navarro, Frenk, & White 1997),

$$\rho_{\text{DM}} = \frac{\delta_c \rho_{\text{crit}}(z) r_s^3}{r(r + r_s)^2}, \quad (13)$$

where

$$\delta_c = \frac{200}{3} \frac{c^3}{[\ln(1+c) - c/(1+c)]}, \quad (14)$$

r_s is the scale radius, c is the concentration parameter, and $\rho_{\text{crit}} = 3H^2/8\pi G$ is the critical density at the redshift z of the cluster. The latter is calculated assuming $\Omega_0 = 0.3$, $\Omega_{\Lambda,0} = 0.7$, and $H_0 =$

Table 1: Parameters used in determining the gravitational potential

Cluster	BCG	r_s (kpc)	c	z	M_B	$B - V$	L_B ($10^{11} L_{B,\odot}$)	R_e (kpc)	M_{bh} ($10^9 M_\odot$)
Virgo	NGC 4486 (M87)	560	2.8	(see below)	-21.96	0.93	0.938	5.03	1.38
Abell 262	NGC 0708	85	8.62	0.0155	-21.08	1.06	0.417	25.6	0.555
Sersic 159-03	ESO 291-009	159	6.56	0.0572	-22.16	1.00	1.13	29.5	1.92
Abell 4059	ESO 349-010	744	2.7	0.0466	-22.73	1.06	1.91	24.5	4.12
Hydra A	PGC 026269	77	12.3	0.0550	-22.97	0.82	2.38	39.6	4.12
Abell 496	PGC 015524	129	7.75	0.0322	-22.48	1.12	1.51	49.9	3.27
Abell 1795	PGC 049005	430	4.21	0.0639	-22.04	1.00	1.01	40.3	1.66
Perseus	NGC 1275	481	4.09	0.0179	-22.62	0.53	1.72	15.3	1.89

The NFW parameters r_s and c describe the clusters’ dark matter density profiles. For Virgo r_s and c are taken from McLaughlin (1999). For Hydra A, r_s and c are taken from David et al (2001). For all other clusters, r_s and c are taken from table 1 of Piffaretti et al (2005). Redshifts z are taken from Kaastra et al (2004), except for Virgo — Kaastra et al (2004) take the distance to Virgo to be 16 Mpc, and we use the same value. Absolute B-band magnitudes M_B and $B - V$ color indices for the brightest cluster galaxies (BCGs) are taken from the “Hyperleda” database of Paturel et al (2003). The BCG effective radii R_e are taken from Schombert (1987) for Perseus and Abell 1795, from Graham et al (1996) for Hydra A, Abell 262, and Abell 496, and from “Hyperleda” for Virgo, Sersic 159-03 and Abell 4059. L_B is the BCG B-band luminosity. The black hole masses are determined using the mass-luminosity relation given in equation (6) of Lauer et al (2007).

$70 \text{ km s}^{-1} \text{ Mpc}^{-1}$. The values of r_s , c , and z for the eight clusters we consider in section 3 are taken from the literature and listed in table 1.

We take the stellar mass density to have a Hernquist profile in which the stellar mass interior to radius r is

$$M_{\text{stars}}(r) = \frac{M_0 r^2}{(r + a)^2}, \quad (15)$$

where M_0 is the total stellar mass and a is a scale length equal to $R_e/1.8153$, where R_e is the radius of the isophote enclosing half the galaxy’s light. (Hernquist 1990) As in Graham et al (2006), we set $M_0 = Y_B L_B$, where L_B is the BCG B-band luminosity, and $Y_B = 5.3 M_\odot / L_{B,\odot}$ is the B-band stellar mass-to-light ratio for a 12-Gyr-old single stellar population (Worthey 1994). We set $L_B / L_{B,\odot} = 10^{0.4(M_{B,\odot} - M_B)}$, where $M_{B,\odot}$ and M_B are, respectively, the solar and BCG absolute B-band magnitudes, and $M_{B,\odot} = 5.47$ (Cox 2000). The values of R_e and M_B for each cluster are taken from the literature (see table 1).

We determine the black-hole mass using the mass-luminosity relation given in equation (6) of Lauer et al (2007):

$$\log \left(\frac{M_{\text{bh}}}{M_{\odot}} \right) = 8.67 - 0.528(M_V + 22), \quad (16)$$

where M_V is the BCG absolute V-band magnitude. We set $M_V = M_B - (B - V)$, where M_B and the $B - V$ color index for each cluster are taken from the “Hyperleda” database (Paturel et al 2003) and listed in table 1. The resulting values of M_{bh} for each cluster are also listed in table 1.

The contribution to the gravitational potential from the intracluster plasma Φ_p is not determined ahead of time, but is instead obtained by solving $\nabla^2 \Phi_p = -4\pi G \langle \rho \rangle$, where $\langle \rho \rangle$ is the average plasma density that results from solving the model equations.

2.4. Radiative cooling and chemical composition

We use the analytic fit of Tozzi & Norman (2001) to approximate the full cooling function for free-free and line emission:

$$R = n_i n_e \left[0.0086 \left(\frac{k_B T}{1 \text{ keV}} \right)^{-1.7} + 0.058 \left(\frac{k_B T}{1 \text{ keV}} \right)^{0.5} + 0.063 \right] \cdot 10^{-22} \text{ ergs cm}^3 \text{ s}^{-1}, \quad (17)$$

where n_i is the ion density, n_e is the electron density, k_B is the Boltzmann constant, and the numerical constants correspond to 30% solar metallicity. Because we treat the turbulent fluctuations as small, we can replace n_e , n_i , and T in equation (17) by their average values when calculating $\langle R \rangle$. We take the intracluster plasma to be fully ionized and to have a uniform chemical composition, with a hydrogen mass fraction of $X = 0.7$ and a helium mass fraction $Y = 0.29$. We take the metals to have a mean charge to mass ratio equal to that of helium. The mean molecular weight is then

$$\mu \equiv \frac{\rho}{(n_e + n_i)m_H} = 0.62. \quad (18)$$

The mean molecular weight per electron is then

$$\mu_e \equiv \frac{\rho}{n_e m_H} = 1.18. \quad (19)$$

In addition,

$$\frac{n_i}{n_e} = 0.91, \quad (20)$$

and

$$\frac{n_e}{n_H} = 1.21, \quad (21)$$

where n_H is the hydrogen number density.

2.5. Transport

Cluster magnetic fields are easily strong enough to cause cosmic rays and heat to diffuse primarily along magnetic field lines, so that

$$\kappa \simeq \kappa_{\parallel} \hat{b} \hat{b}, \quad (22)$$

and

$$D \simeq D_{\parallel} \hat{b} \hat{b}, \quad (23)$$

where \hat{b} is the magnetic field unit vector, and κ_{\parallel} and D_{\parallel} are the parallel conductivity and diffusivity. We take the parallel conductivity to be the classical Spitzer thermal conductivity (Spitzer & Harm 1953, Braginskii 1965),

$$\kappa_{\parallel} = \kappa_S = 9.2 \times 10^{30} n_e k_B \left(\frac{k_B T}{5 \text{ keV}} \right)^{5/2} \left(\frac{10^{-2} \text{ cm}^{-3}}{n_e} \right) \left(\frac{37}{\ln \Lambda_c} \right) \frac{\text{cm}^2}{\text{s}}, \quad (24)$$

where $\ln \Lambda_c$ is the Coulomb logarithm. The local anisotropy of κ and D turns out to be critical for convective stability, as discussed by Balbus (2000,2001), Parrish & Stone (2005,2007), Chandran & Dennis (2006), and Rasera & Chandran (2007), and we take this anisotropy into account in our mixing length theory for intracluster convection. [See, e.g., the discussion preceding equation (B29).] However, when we average equations (2) through (5) and solve for the structure of the ICM, we are interested in the transport of heat and cosmic rays over distances much greater than the correlation length of the magnetic field, l_B , which is $\sim 1 - 10$ kpc (Kronberg 1994; Taylor et al 2001, 2002; Vogt & Ensslin 2003, 2005 - see Schekochihin et al 2006 and Schekochihin & Cowley 2006 for a recent discussion of intracluster magnetic fields and turbulence). For transport over such large scales, averaging over the turbulent magnetic field leads to an effectively isotropic conductivity, which we denote κ_T , that is reduced relative to κ_{\parallel} (Rechester & Rosenbluth 1978, Chandran & Cowley 1998). Theoretical studies find that the reduction is by a factor of $\sim 5 - 10$ (Narayan & Medvedev 2001, Chandran & Maron 2004, Maron, Chandran, & Blackman 2004). In this paper, we assume that

$$\kappa_T = \frac{\kappa_{\parallel}}{8}. \quad (25)$$

We take the average of the conductive heating term to be given by

$$\langle \nabla \cdot (\kappa \cdot \nabla T) \rangle = \frac{1}{r^2} \frac{d}{dr} \left[r^2 \kappa_T \frac{d}{dr} \langle T \rangle \right], \quad (26)$$

with T set equal to $\langle T \rangle$ in equation (24). Similarly, we assume that

$$\langle \nabla \cdot (D \cdot \nabla p_{\text{cr}}) \rangle = \frac{1}{r^2} \frac{d}{dr} \left[r^2 D_{\text{cr}} \frac{d}{dr} \langle p_{\text{cr}} \rangle \right]. \quad (27)$$

We take the value of D_{cr} to be

$$D_{\text{cr}} = \sqrt{D_0^2 + v_d^2 r^2}, \quad (28)$$

where $D_0 = 10^{28} \text{ cm}^2/\text{s}$ and $v_d = 10 \text{ km/s}$. The v_d term is loosely motivated by a simplified picture of cosmic-ray “self-confinement,” in which cosmic rays are scattered by waves generated by the streaming of cosmic rays along field lines. If, contrary to fact, the field lines were purely radial, efficient self-confinement would limit the average radial velocity of the cosmic rays to the Alfvén speed v_A , allowing the cosmic rays to travel a distance r in a time $\sim r/v_A$. For constant v_A , this scaling can be approximately recovered by taking the cosmic rays to diffuse isotropically with $D_{\text{cr}} \propto r$, the scaling that arises from equation (28) when $v_d r \gg D_0$. This self-confinement scenario is too simplistic, since in clusters field lines are tangled, v_A varies in space, and it is not known whether cosmic rays are primarily scattered by cosmic-ray-generated waves or by magnetohydrodynamic (MHD) turbulence excited by large-scale stirring of the intracluster plasma. It is not clear, however, how to improve upon equation (28). Self-confinement in the presence of tangled field lines is not well understood, and the standard theoretical treatment of scattering by MHD turbulence, which takes the fluctuations to have wave vectors directed along the background magnetic field, is known to be inaccurate (Bieber et al 1994, Chandran 2000, Yan & Lazarian 2004). A more definitive treatment must thus await further progress in our understanding of MHD turbulence and cosmic-ray transport. The value of D_{\parallel} is needed in the mixing length theory developed below. We assume that $D_{\text{cr}}/D_{\parallel} = \kappa_T/\kappa_{\parallel}$, and thus set

$$D_{\parallel} = 8D_{\text{cr}}. \quad (29)$$

2.6. The mass accretion rate and cosmic-ray luminosity of the central AGN

We assume that the black hole at $r = 0$ in our model, with a mass M_{BH} given by equation (16), accretes intracluster plasma at the Bondi (1952) rate,

$$\dot{M} = \frac{\pi G^2 M_{\text{BH}}^2 \rho}{c_s^3}, \quad (30)$$

where c_s is the adiabatic sound speed, and ρ and c_s are evaluated using the average plasma parameters at the radius $r_1 = 0.2 \text{ kpc}$, which defines the inner boundary of our model solutions. We assume that this accretion powers a jet that leads to shocks, which in turn accelerate cosmic rays. We take the cosmic-ray luminosity to be

$$L_{\text{cr}} = \eta \dot{M} c^2, \quad (31)$$

where

$$\eta = 5 \times 10^{-3}. \quad (32)$$

An argument against Bondi accretion in clusters is that the radiative luminosities of AGNs in elliptical galaxies are typically several orders of magnitude smaller than the nominal Bondi accretion power, given by $P_{\text{Bondi}} = 0.1 \dot{M}_{\text{Bondi}} c^2$, where \dot{M}_{Bondi} is the Bondi accretion rate given in equation (30). (Allen et al 2006) However, the mechanical luminosities L_{mech} of these AGN are often much larger than their radiative luminosities. Moreover, in a recent study of nine AGNs in nearby x-ray luminous elliptical galaxies, Allen et al (2006) found a strong correlation between P_{Bondi} (as calculated from the observed plasma temperature and density profiles) and L_{mech} (as inferred from the energies and time scales required to inflate the observed x-ray cavities). Allen et al (2006) found that L_{mech} can be related to P_{Bondi} by a power-law fit of the form $\log(P_{\text{Bondi}}/10^{43} \text{ erg s}^{-1}) = c_1 + c_2 \log(L_{\text{mech}}/10^{43} \text{ erg s}^{-1})$, with $c_1 = 0.65 \pm 0.16$ and $c_2 = 0.77 \pm 0.20$, and that the fraction of $\dot{M}c^2$ that is converted into mechanical luminosity ranges from 1.3% for a jet power of 10^{42} erg/s to 3.7% for a jet power of 10^{44} erg/s . Results consistent with these were also found by Tan & Blackman (2005). These authors reviewed studies of M87 and estimated that L_{mech} is about an order of magnitude larger than the radiative luminosity, and that $L_{\text{mech}} \sim 0.01 \dot{M}_{\text{Bondi}} c^2$. Our choice of $\eta = 0.005$ is smaller than the accretion efficiencies found in these studies, in part to provide a more conservative estimate, and in part because only part of the mechanical energy is converted into cosmic rays.

We note that Bondi accretion in clusters has been considered previously by a number of authors (e.g., Quataert & Narayan 2000, Di Matteo et al 2002, Nulsen 2004, Böhringer et al 2004, Springel et al 2005, Cattaneo & Teyssier 2007). Also, in Tan & Blackman’s (2005) analysis, part of the reason for the small value of η is that part of the mass flowing in through the Bondi radius never reaches the central black hole because it forms stars in a gravitationally unstable disk. Thus, the Bondi accretion rate in our model may be significantly higher than the time derivative of the mass of the central black hole.

Pizzolato & Soker (2005) and Soker (2006) considered a different “cold feedback” scenario for mass accretion, in which cold gas fuels the central AGN. In section 5 we address several issues related to the question of whether one expects Bondi accretion or some form of cold feedback in clusters.

2.7. Cosmic-ray acceleration by the central radio source

The spatial distribution of cosmic-ray injection into the ICM is not precisely known. Some clues are provided by radio observations, which show that cluster-center radio sources (CCRS) differ morphologically from radio sources in other environments. As discussed by Eilek (2004), roughly half of the CCRS in a sample of 250 sources studied by Owen & Ledlow (1997) are “amorphous,” or quasi-isotropic, presumably due to jet disruption by the comparatively high-pressure,

high-density cluster-core plasma. With the exception of Hydra A, the CCRS in the Owen-Ledlow (1997) study are smaller than non-cluster-center sources, with most extending less than 50 kpc from the center of the host cluster (Eilek 2004). Given these findings, we take the cosmic-ray acceleration to be concentrated within the cluster core.

In paper II, it was assumed that the cosmic rays are accelerated in an approximately volume-filling manner. In contrast, in this paper, it is assumed that cosmic-ray energy is injected into the intracluster medium in only a fraction of the volume at any given radius. We then take

$$\dot{E}_{\text{source}} = \langle \dot{E}_{\text{source}} \rangle + \delta \dot{E}_{\text{source}}, \quad (33)$$

where

$$\langle \dot{E}_{\text{source}} \rangle = S_0 e^{-r^2/r_{\text{source}}^2} \quad (34)$$

can be thought of as an average of \dot{E}_{source} over spherical polar angles. The constant r_{source} is a free parameter that characterizes the size of the cosmic-ray acceleration region. The constant S_0 is determined on energy grounds from the equation $L_{\text{cr}} = 4\pi \int_0^\infty dr r^2 \langle \dot{E}_{\text{source}}(r) \rangle$ and equation (31). After determining $\langle \dot{E}_{\text{source}}(r) \rangle$, we set

$$\delta \dot{E}_{\text{rms}} = \eta_2 \langle \dot{E}_{\text{source}} \rangle, \quad (35)$$

where $\delta \dot{E}_{\text{rms}}$ is the rms value of $\delta \dot{E}_{\text{source}}$, and η_2 is a constant that is related to the volume filling factor of the cosmic-ray acceleration region. For example, suppose that $\dot{E}_{\text{source}} = C = \text{constant}$ in a fraction f_{cr} of the volume between radius r and $r + dr$, and that $\dot{E}_{\text{source}} = 0$ in the remainder of the volume between r and $r + dr$. In this case, $\langle \dot{E}_{\text{source}}(r) \rangle = f_{\text{cr}} C$, $\langle [\dot{E}_{\text{source}}]^2 \rangle = f_{\text{cr}} C^2$, and $\delta \dot{E}_{\text{rms}} = \sqrt{\langle [\dot{E}_{\text{source}}(r) - \langle \dot{E}_{\text{source}}(r) \rangle]^2 \rangle} = \langle \dot{E}_{\text{source}}(r) \rangle \sqrt{f_{\text{cr}}^{-1} - 1}$. For the calculations presented below, we set $\eta_2 = 2.5$, which corresponds to $f_{\text{cr}} = 0.138$. These fluctuations in the cosmic-ray source term drive fluctuations in the fluid quantities and contribute to convection. This effect is incorporated into the two-fluid mixing length theory presented in appendix B. The fluctuations in \dot{E}_{source} result in larger fluctuations (spatial variations) in p_{cr} and ρ than in the model of paper II, which in some sense represent the “cosmic-ray bubbles” or X-ray cavities seen in about one-fourth of the clusters in the Chandra archive (Birzan et al 2004).

2.8. Summary and numerical method

The approximations described above lead to a set of coupled ordinary differential equations for the average density, temperature, and cosmic-ray pressure and the rms turbulent velocity. These equations are presented in appendix B. We solve this set of equations using a shooting method, in which we guess the electron density, temperature, and cosmic-ray pressure at the inner radius of

our model ($r_1 = 0.2$ kpc) and then update these guesses until the model solution satisfies the three boundary conditions at the outer radius r_{outer} . These outer boundary conditions are the observed electron density $n_{e,\text{outer}}$ and temperature T_{outer} at r_{outer} , and a condition on $\langle dp_{\text{cr}}/dr \rangle$ at r_{outer} , which amounts to requiring that $\langle p_{\text{cr}} \rangle \rightarrow 0$ as $r \rightarrow \infty$. The value of r_{outer} for a cluster is taken to be the radius of the first observational data point outside the cluster’s cooling radius, r_{cool} , given in table 2 (except for Virgo, for which we take r_{outer} to be the outermost data point, which lies inside of r_{cool} .) The values of r_{outer} , n_{outer} , and T_{outer} are listed in table 3. After finding the values of n_e , T , and p_{cr} at r_1 needed to match the boundary conditions at r_{outer} , we integrate the equations out to radii greater than r_{outer} as needed to compare to the data. A more extensive discussion of our numerical method is given in appendix B.

3. Comparison to observations

We compare our model solutions with observations of the central regions ($r < 0.25r_{\text{vir}}$, where $r_{\text{vir}} = cr_s$ is the virial radius) of eight clusters: Virgo, Abell 262, Sersic 159-03, Abell 4059, Hydra A, Abell 496, Abell 1795, and Perseus. Temperature and hydrogen-number-density (n_H) profiles for these clusters are taken from table 5 of Kaastra et al (2004). Redshifts (z) and angular-diameter distances d_{scdm} are given in table 1 of Kaastra et al (2004). The data of Kaastra et al (2004) are obtained assuming a standard cold dark matter (SCDM) cosmology with $\Omega = 1$ and $H_0 = 50 \text{ km s}^{-1} \text{ Mpc}^{-1}$. We convert to a Λ CDM cosmology with $\Omega_0 = 0.3$, $\Omega_{\Lambda,0} = 0.7$, and $H_0 = 70 \text{ km s}^{-1} \text{ Mpc}^{-1}$ by calculating the ratio of angular-diameter distance in the two cosmologies, $\zeta(z) \equiv d_{\text{scdm}}/d_{\Lambda\text{cdm}}$, for each cluster in the sample. We then multiply Kaastra et al’s (2004) values for n_H by $\sqrt{\zeta}$ (since the observed X-ray flux and angular size are fixed) and multiply linear distances by ζ^{-1} . Values of ζ , as well as the cooling radius, are given in table 2. [The conversion from n_H to n_e is given by equation (21).]

We adjust a single parameter, r_{source} , to fit to the observations. The optimal values for r_{source} are given in table 3. The temperature and density profiles in the model solutions are plotted in figures 1 and 2. We note that the central peak in the Perseus temperature data is due to the hard power-law spectrum of the central active galaxy NGC 1275 (E. Churazov, private communication). The values of \dot{M} and L_{cr} , as well as fluid quantities at $r_1 = 0.2$ kpc and r_{outer} are given in table 3. The radial profiles of the rms turbulent velocity and cosmic-ray pressure are presented in appendix A.

Overall, the model profiles match the observations quite well, which suggests that convection is an important process in cluster cores. The model, however, substantially underestimates the observed density in Sersic 159-03 at $r \lesssim 50$ kpc. This discrepancy may be explained by a recent study by Werner et al (2007). These authors found that Sersic 159-03 has the largest soft x-ray excess of all clusters observed by XMM-Newton and argued that the observed excess is best explained by

Table 2: Cluster parameters

Cluster	$\frac{d_{\text{scdm}}}{d_{\Lambda\text{cdm}}}$	r_{cool} (kpc)
Virgo	1.0	73
Abell	1.39	61
Sersic 159-03	1.36	128
Abell 4059	1.37	86
Hydra A	1.36	130
Abell 496	1.38	89
Abell 1795	1.36	130
Perseus	1.39	128

The quantity d_{scdm} is the angular-diameter distance to each cluster in the SCDM cosmology employed by Kaastra et al (2004) in which $\Omega = 1$ and $H_0 = 50 \text{ km s}^{-1} \text{Mpc}^{-1}$. $d_{\Lambda\text{cdm}}$ is angular-diameter distance to each cluster in the ΛCDM cosmology assumed in this paper, in which $\Omega = 0.7$, $\Omega_\Lambda = 0.3$ and $H_0 = 70 \text{ km s}^{-1} \text{Mpc}^{-1}$. For Virgo, $d_{\text{scdm}}/d_{\Lambda\text{cdm}}$ is set equal to 1.0, since we use the same distance (16 Mpc) to Virgo as employed by Kaastra et al (2004). The cooling radii r_{cool} are taken from Kaastra et al (2004) but rescaled to ΛCDM . Kaastra et al’s values of r_{cool} are the radii at which the radiative cooling time t_{cool} is 15 Gyr in SCDM. At the rescaled values of r_{cool} , t_{cool} is $15 \text{ Gyr} \cdot (d_{\Lambda\text{cdm}}/d_{\text{scdm}})^{1/2}$ in ΛCDM (because the cooling time scales like n_e^{-1} and $n_e \propto d^{-1/2}$ for a fixed observed X-ray flux and angular size, where d is the angular-diameter distance).

the presence of a substantial population of non-thermal electrons that is concentrated in the cluster core. When they modeled the observed emission as coming from a combination of thermal plasma and nonthermal electrons, they found that the x-ray emission between 0.3 and 10 keV from non-thermal electrons is a substantial fraction of the emission from the thermal plasma at large radii ($\sim 35 - 55\%$ at $r \simeq 375 \text{ kpc}$) but only a small fraction of the emission at small radii ($\sim 1 - 7\%$ at $r \lesssim 50 \text{ kpc}$). Thus, the non-thermal contribution to the emission measure does not lead directly to a large change in the observationally inferred electron density at $r \lesssim 50 \text{ kpc}$. On the other hand, Werner et al (2007) note that if there is a non-thermal proton population with significantly more pressure than the non-thermal electrons, the total cluster mass may be significantly underestimated. Moreover, since the non-thermal pressure inferred by Werner et al (2007) peaks strongly towards the cluster’s center, the actual gravitational acceleration in the central 50-100 kpc may be much larger than in an NFW profile calculated neglecting non-thermal pressure. This is an issue for all the clusters that we consider, but especially for Serisc 159-03, since its especially large soft excess indicates a large non-thermal pressure fraction. We note that although the non-thermal emission

is less peaked than the thermal emission in the results of Werner et al (2007) (i.e., $p_{\text{non-thermal}}/n_e^2$ decreases towards the center), the non-thermal pressure is more peaked than the thermal pressure ($p_{\text{non-thermal}}/p$ increases inwards). If we were to re-calculate our model solutions using a larger gravitational acceleration in the cluster core, the thermal plasma density would peak more sharply near the cluster center than in Figure 1. Thus, the deviation between the model and observations of Sersic 159-03 may be due to a significant underestimate of the gravitational acceleration in this cluster resulting from its unusually large non-thermal pressure.

Table 3: Physical quantities in the model solutions

Cluster	r_{source} (kpc)	$n_e(r_1)$ (cm^{-3})	$k_B T(r_1)$ (keV)	$\frac{p_{\text{cr}}(r_1)}{p(r_1)}$	$\frac{ \langle v_r(r_1) \rangle }{c_s(r_1)}$	\dot{M}_{Bondi} ($M_\odot \text{yr}^{-1}$)	L_{cr} (erg/s)	r_{outer} (kpc)	$k_B T_{\text{outer}}$ (keV)	$n_{e,\text{outer}}$ (cm^{-3})
Virgo	1.70	0.115	1.27	0.268	0.00207	0.00203	5.77×10^{41}	49.3	2.50	2.85×10^{-3}
Abell 262	34.0	0.231	0.118	0.153	0.0388	0.0232	6.59×10^{42}	93.6	2.16	1.22×10^{-3}
Sersic 159-03	46.0	0.397	0.133	1.24	0.365	0.399	1.13×10^{44}	165	2.38	1.35×10^{-3}
Abell 4059	24.0	0.168	0.727	0.156	0.0562	0.0607	1.72×10^{43}	137	3.89	1.75×10^{-3}
Hydra A	35.0	0.742	0.340	0.740	0.257	0.839	2.38×10^{44}	160	3.28	2.05×10^{-3}
Abell 496	5.00	0.0437	0.965	0.701	0.0201	0.00650	1.85×10^{42}	96.2	3.93	2.53×10^{-3}
Abell 1795	40.0	0.671	0.165	0.700	0.177	0.363	1.03×10^{44}	184	5.56	2.19×10^{-3}
Perseus	16.0	2.47	0.487	0.121	0.0264	0.343	9.75×10^{43}	162	5.27	2.16×10^{-3}

r_{source} is the size of the cosmic-ray acceleration region that leads to the best fit between the mixing-length model and the observations of Kaastra et al (2004). $n_e(r_1)$, $T(r_1)$, $p(r_1)$, and $p_{\text{cr}}(r_1)$ are the electron density, temperature, thermal pressure, and cosmic-ray pressure at the inner radius $r_1 = 0.2$ kpc. v_r and c_s are the radial velocity and adiabatic sound speed. \dot{M}_{Bondi} is the Bondi accretion rate based on the plasma density and plasma temperature at $r = r_1$, and $L_{\text{cr}} = 0.005 \dot{M}_{\text{Bondi}} c^2$ is the cosmic-ray luminosity of the central radio source. T_{outer} and $n_{e,\text{outer}}$ are the observed temperature and electron density at the radius r_{outer} of the outer boundary used in our shooting method.

One of the quantities that is calculated as part of our solutions is the cosmic-ray luminosity L_{cr} of the central AGN. To further test the plausibility of our model, we compare the theoretically predicted values of L_{cr} from table 3 and the observationally inferred mechanical luminosity L_{mech} of the central AGN in the six clusters in our sample for which we were able to find published values. The mechanical luminosities are taken from Bîrzan et al (2004), and are calculated from observations of X-ray cavities, by assuming that an energy pV (where p is the surrounding pressure and V is the cavity volume) per cavity is released during a time equal to the buoyancy time scale. We plot L_{mech} versus L_{cr} in figure 3. The error bars in this figure take into account projection effects on the estimate of the cavity volume as well as uncertainties in the ages of the cavities. These two

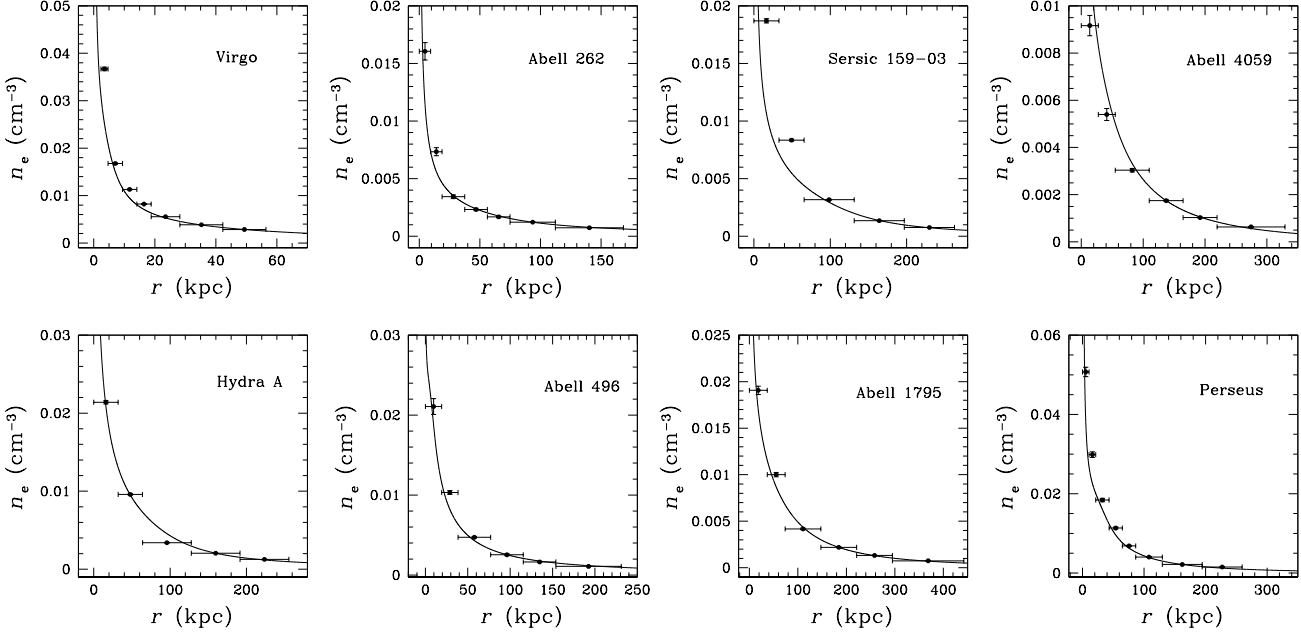


Fig. 1.— The solid lines give the electron density as a function of radius in our model solutions for the eight clusters in our sample. The data points are from the observations of Kaastra et al (2004).

luminosities are strongly correlated over a range of $\sim 100 - 1000$ in luminosity.

4. The energy budget of the intracluster medium

In our model, radiative cooling is balanced by a combination of thermal conduction, convective heating, and radial inflow due to the accretion onto the central AGN. To distinguish between these last two mechanisms, we separate the average radial velocity into two components,

$$\langle v_r \rangle = v_{\text{inflow}} + v_{r,\text{turb}}, \quad (36)$$

where

$$v_{\text{inflow}} = -\frac{\dot{M}}{4\pi r^2 \langle \rho \rangle} \quad (37)$$

is the inflow rate that arises in a laminar radial flow with constant mass accretion rate \dot{M} . The term $v_{r,\text{turb}}$ is an additional average radial velocity that is induced by the convection. [Its value is given by $-\langle \delta \rho \delta v_r \rangle / \langle \rho \rangle$, as in equation (B5).] With this definition in hand, we write the average of equation (4), divided by $(\gamma - 1)$, as

$$0 = \langle H_{\text{inflow}} + H_{\text{conv}} + H_{\text{visc}} + H_{\text{tc}} - R \rangle. \quad (38)$$

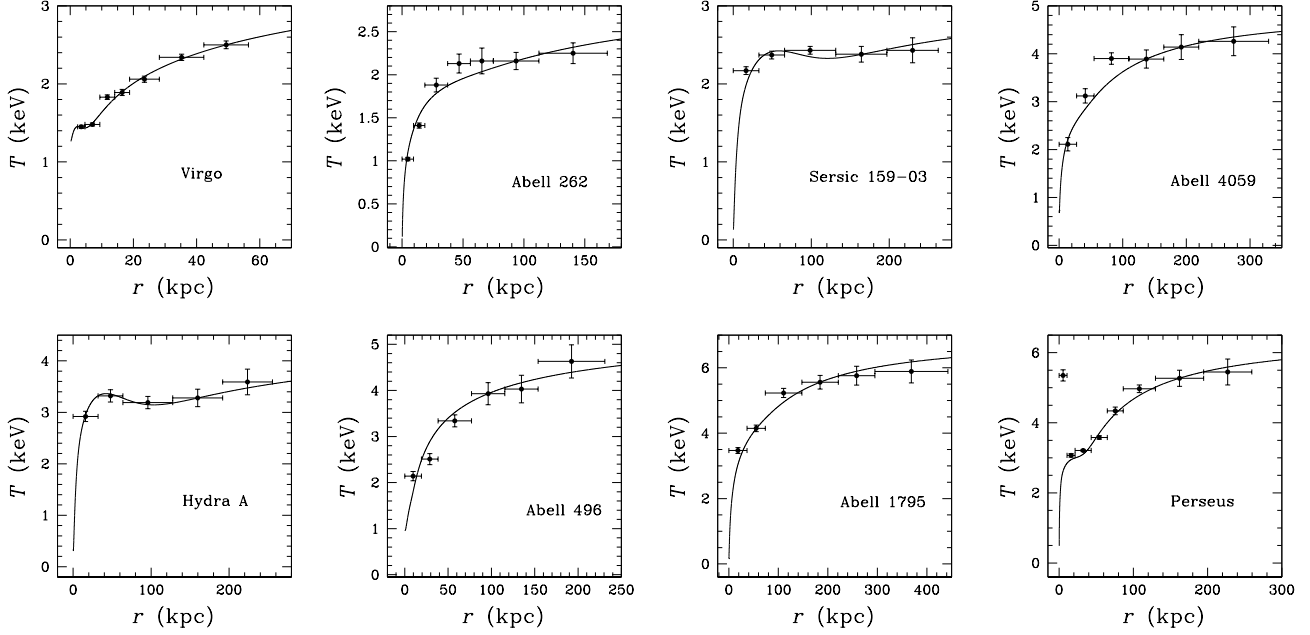


Fig. 2.— The solid lines give the temperature as a function of radius in our model solutions for the eight clusters in our sample. The data points are from the observations of Kaastra et al (2004).

Here,

$$\langle H_{\text{inflow}} \rangle = -\frac{1}{(\gamma-1)r^2} \frac{d}{dr} (r^2 v_{\text{inflow}} \langle p \rangle) - \frac{\langle p \rangle}{r^2} \frac{d}{dr} (r^2 v_{\text{inflow}}) \quad (39)$$

is the source term associated with v_{inflow} . The term

$$\langle H_{\text{conv}} \rangle = \left\langle -\frac{\nabla \cdot (vp)}{(\gamma-1)} - p \nabla \cdot v - H_{\text{inflow}} \right\rangle \quad (40)$$

is the convective heating rate of the thermal plasma, excluding viscous dissipation. It includes the turbulent diffusion of heat as well as the turbulent pdV work done on the thermal plasma by cosmic rays. The average of the viscous dissipation term is set equal to

$$\langle H_{\text{visc}} \rangle = \frac{0.42 \rho u_{\text{rms}}^3}{l}, \quad (41)$$

where $l = 0.4r$ is the mixing length, u_{rms} is the rms turbulent velocity defined in equation (B71), and the constant 0.42 is taken from direct numerical simulations of compressible magnetohydrodynamic turbulence (Haugen, Brandenburg, & Dobler 2004).¹ The average of H_{ic} is given by equation (26), and the average of R is given by equation (17).

¹The constant 0.42 is obtained by taking the mixing length l to correspond to π/k_p in the simulations of Haugen et al (2004), where k_p is the wave number at which $kE(k)$ peaks, and $E(k)$ is the power spectrum of the turbulent velocity.

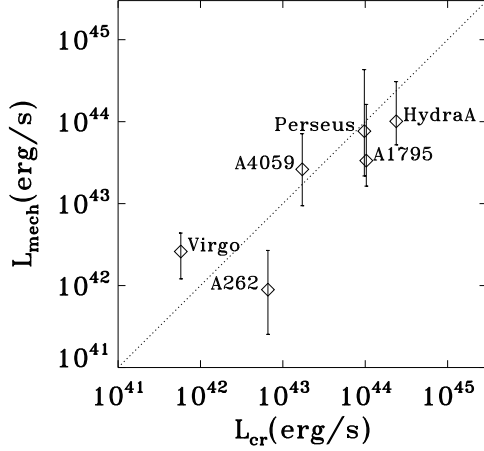


Fig. 3.— Comparison between the cosmic-ray luminosities in our model calculations L_{cr} against observationally inferred values of the mechanical luminosities of the central AGN in six of the clusters in our sample (Bîrzan et al 2004). The dotted line represents equality between these two quantities.

In figure 4, we plot the averages of H_{inflow} (dotted line), H_{conv} (long-dashed line), H_{tc} (short-dashed line), and R (solid line), integrated over volume from the inner radius of our model ($r_1 = 0.2$ kpc) out to radius r . We find that $\langle H_{\text{visc}} \rangle \ll \langle H_{\text{conv}} \rangle$ everywhere in each cluster, and so we omit H_{visc} from the figures to keep the plots easier to read.²

We can divide the clusters into two groups, those with AGN-dominated heating and those with conduction-dominated heating. In Hydra A and Sersic 159-03, the heating within the central 100 kpc is dominated by convection driven by the central AGN. In all of the other clusters, the heating within the central 100 kpc is dominated by thermal conduction. The inability of conduction to balance cooling in Hydra A and Sersic 159-03 was previously noted by Zakamska & Narayan (2003). These authors constructed density and temperature profiles for clusters assuming that radiative cooling is balanced by conductive heating, setting the thermal conductivity equal to a constant f_c times the Spitzer thermal conductivity. For Hydra A and Sersic 159-03, they found that the values of f_c that best fit the observations were 1.5 and 5.6, respectively, much larger than the theoretically expected value of $f_c \simeq 0.1 - 0.2$. In contrast, for Abell 1795 the best-fit value of f_c was 0.2.

²We note that equation (38) is not exactly satisfied by our model solutions. In our model, we use the total-energy equation [equation (B3)] instead of the plasma energy [equation (4)]. Although equation (4) is exactly satisfied when equations (B3), (3), and (5) are satisfied, our mixing-length approximation of the average of equation (4) is not exactly satisfied when our mixing-length approximations to the averages of equations (B3), (3), and (5) are satisfied. This discrepancy is noticeable at the largest radii in Hydra A and Sersic 159-03.

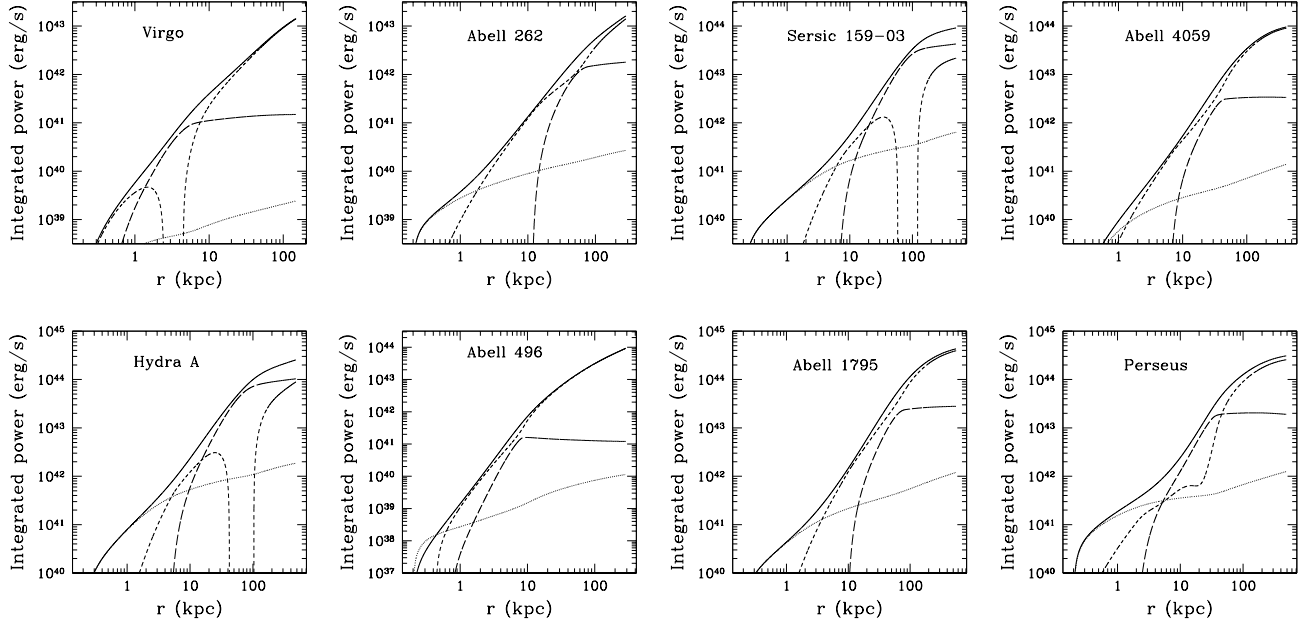


Fig. 4.— The energy sources and sinks in the thermal plasma, integrated over volume from the inner radius $r_1 = 0.2$ kpc out to radius r . The solid line is the radiative losses (X-ray luminosity), the short dashed line is the heating from thermal conduction, the dotted line is power contributed by the inflow associated with the mass accretion rate, and the long-dashed line is the heating power due to the convective turbulence, which includes both the turbulent diffusion of heat and $p dV$ work by cosmic-rays.

What are the characteristics of a cluster that determine whether AGN feedback or thermal conduction is the dominant heat source within the central 100 kpc? Given that $\kappa_S \propto T^{5/2}$, it seems clear that a lower average temperature T_{avg} makes thermal conduction less able to balance radiative cooling, leading in turn to a relatively greater role for AGN feedback. However, although T_{avg} is important for determining the relative strength of conduction and AGN feedback, on its own the value of T_{avg} does not explain our results, since Virgo and Abell 262 have temperatures comparable to that of Seric 159-03 and lower than that of Hydra A. An equally important factor appears to be the baryon density in the core. In particular, the clusters with AGN-dominated heating are significantly denser at a given radius than clusters with conduction-dominated heating that have similar average temperatures. For example, for radii between 20 and 50 kpc, the electron density in Seric 159-03 is 2-3 times greater than in Virgo. Similarly, at $r = 100$ kpc the electron density in Hydra A is $\sim 60\%$ larger than in Abell 4059,³ even though Abell 4059 has a higher average temperature and larger virial mass. (Typically, at a fixed radius the density is larger in hotter,

³This ratio is based on the model density profile due to the offset in the radius of the observed densities, but a similar conclusion is reached by interpolating between data points.

more massive clusters.) It thus appears that the clusters in which AGN feedback dominates most strongly over conduction are those in which the clusters’ ongoing formation channels unusually large quantities of baryons towards the clusters’ cores.

We conclude this section with a few additional comments relating to figures 3 and 4. Bîrzan et al (2004) found that their observationally inferred values of L_{mech} for 16 clusters were correlated with the X-ray luminosity inside the cooling radius r_{cool} , denoted L_X , supporting the idea that AGN feedback is at least part of the solution to the cooling-flow problem. However, the level of the mechanical luminosity in their study turns out to be a factor of 1 to 20 lower than the X-ray luminosity, which raises the question of whether the mechanical luminosity is sufficient to offset cooling in these clusters. Our model solutions and figure 3 show that the mechanical luminosity is indeed sufficient when thermal conduction is also accounted for, and our discussion above regarding AGN-dominated heating versus conduction-dominated heating offers an explanation for the large variations in the ratio L_X/L_{mech} . When heating is dominated by conduction, AGN feedback heating is only a small fraction of the power radiated from within the cooling radius, and L_X/L_{mech} is large. On the other hand, when AGN-driven convection dominates the heating, the AGN heating power is similar to the total power radiated from within r_{cool} , and $L_X \sim L_{\text{mech}}$.

We note that figure 4 shows that in Hydra A, Sersic 159-03, and Virgo, conduction actually acts to cool the plasma over a limited range of r due to the local maximum in the temperature profile. Also, in none of the clusters is the total convective heating rate equal to L_{cr} . This is because the cosmic-ray luminosity is the power deposited into the cosmic-ray fluid, and only part of this is transferred to the thermal plasma through pdV work. Additional plasma heating arises from the redistribution (turbulent diffusion) of plasma thermal energy resulting from the convective motions. As can be seen from figure 4 and table 3, the total convective heating of the thermal plasma is typically on the order of one-third of L_{cr} .

5. Clusters with central cooling flows

An important point to emerge from figure 4 is the appearance of central cooling flows in several clusters - Abell 262, Sersic 159-03, Hydra A, Abell 1795, and Perseus - with radii r_{cf} that are typically a few kpc. Heating is unable to balance cooling at $r < r_{\text{cf}}$ in these clusters for several reasons: the AGN feedback heating is distributed over a large volume, thermal conduction becomes less efficient at small r due to the lower temperatures and the fact that $\kappa_T \propto T^{5/2}$, and the radiative losses per unit volume peak sharply at small r due to the large plasma densities. As a result, a cooling flow develops in which the energy lost to cooling is replenished by the inflow. Within this central region, we have the approximate relation $t_{\text{cool}} \sim t_{\text{inflow}}$, where $t_{\text{inflow}} = r/|v_{\text{inflow}}|$ is the inflow time and $t_{\text{cool}} = 1.5nk_B T/R$ is the local cooling time. Because $t_{\text{inflow}} \sim t_{\text{cool}}$, the mass

accretion rate at $r = r_{\text{cf}}$ is approximately given by

$$\dot{M} \sim 4\pi r_{\text{cf}}^2 \rho(r_{\text{cf}}) \left[\frac{r_{\text{cf}}}{t_{\text{cool}}(r_{\text{cf}})} \right] \sim \frac{M_{\text{cf}}}{t_{\text{cool}}(r_{\text{cf}})}, \quad (42)$$

where r_{cf} is the radius of the central cooling flow region, and M_{cf} is the mass of plasma contained within the cooling flow region. Because we have no sources or sinks of plasma, \dot{M} is independent of r in our model.

How do these central cooling flows match onto adiabatic Bondi flow at smaller radii? In our model, as r decreases from r_{cf} towards zero, ρ rises and T decreases until the Bondi accretion rate at the fixed radius $r_1 = 0.2$ kpc matches the cooling-flow mass accretion rate given by equation (42). However, our forcing the flow to become adiabatic at r_1 is artificial, and leads to an unrealistic plasma profile near r_1 with an abrupt transition in the flow at r_1 . A better approach was adopted by Quataert & Narayan (2000). These authors investigated radial inflow with cooling in the absence of thermal conduction and cosmic rays using a numerical shooting method and solved all the way in to the sonic point, $r = r_{\text{sonic}}$, at which $v_r = -c_s$. They found a smooth transition from an outer cooling flow with $t_{\text{inflow}} \simeq t_{\text{cool}}$ to an inner adiabatic Bondi flow with $t_{\text{inflow}} \ll t_{\text{cool}}$, provided that $r_{\text{sonic}} \lesssim r_{\text{tr}}$, where

$$r_{\text{tr}} \equiv \frac{GM_{\text{bh}}}{\sigma^2} = 0.05 \text{ kpc} \left(\frac{M_{\text{bh}}}{10^9 M_{\odot}} \right) \left(\frac{\sigma}{300 \text{ km/s}} \right)^{-2} \quad (43)$$

is the radius within which gravity is dominated by the black hole and σ is the circular velocity of the BCG, which was taken to be independent of r . They also found that equation (42) was an accurate estimate of the numerically calculated mass accretion rate in the absence of mass dropout. For $r_{\text{sonic}} < r_{\text{tr}}$, Quataert & Narayan's solution satisfies $c_s \sim \sigma = \text{constant}$ at $r > r_{\text{tr}}$. In the absence of mass dropout, the condition $t_{\text{cool}} = t_{\text{inflow}}$ leads to the relation $\rho \propto r^{-3/2}$ within the cooling-flow part of their solution. The Bondi accretion rate \dot{M}_{Bondi} [given by equation (30)] evaluated at a radius r within the cooling-flow part of their solution thus increases towards smaller r like $r^{-3/2}$. At a sufficiently small value of r , which we call r_{ad} , the Bondi accretion rate equals the rate \dot{M}_{cf} at which mass flows in through the cooling flow, and the flow makes a transition to an adiabatic Bondi flow. At $r < r_{\text{ad}}$, the ratio $t_{\text{cool}}/t_{\text{inflow}}$ increases towards smaller r , and so the neglect of cooling at $r < r_{\text{ad}}$ is self-consistent. We note that the Bondi accretion formula can be applied in the model of Quataert & Narayan (2000) at the outer boundary of the adiabatic flow region, r_{ad} , even if r_{ad} lies outside the region in which the black hole dominates the gravitational acceleration. This is because the Bondi accretion rate depends only on the specific entropy s of the plasma and M_{bh} , and s is constant for $r < r_{\text{ad}}$.

It would be valuable to incorporate into our model an approach similar to that of Quataert & Narayan (2000), including cosmic rays, thermal conduction, and the possibility of convection. Although such a calculation is beyond the scope of this paper, we expect that in such an analysis

the mass accretion rate of the central accretion flow and the plasma parameters at r_{Bondi} are still controlled by \dot{M}_{cf} , as in Quataert & Narayan’s (2000) work. Because the central accretion flow is in some sense slaved to the surrounding cooling flow, the AGN regulates the mass accretion rate primarily by controlling the properties of the central cooling flow, and in particular by controlling r_{cf} . For example, if \dot{M} rises above the equilibrium value, the AGN-feedback heating rises. This then reduces r_{cf} , because one has to go to smaller r in order for ρ to rise enough that cooling exceeds the convective heating rate. The reduction in r_{cf} reduces \dot{M} , as can be seen from equation (42), which then causes \dot{M} to drop back down to its equilibrium level.

As mentioned above, the existence of a smooth transition from a cooling flow to an inner adiabatic Bondi flow requires that $r_{\text{sonic}} < r_{\text{tr}}$. Otherwise, as described by Quataert & Narayan (2000), the ratio $t_{\text{cool}}/t_{\text{inflow}}$ decreases inwards in the supersonic region at $r_{\text{tr}} < r < r_{\text{sonic}}$, and the plasma cools rapidly to very low temperature. In this case, the cooling plasma could still end up fueling the central black hole, but it would do so through some process other than the one we have assumed in our model, e.g., by forming stars whose winds then feed the black hole or through infalling cold gas [see, e.g., Pizzolato & Soker (2005) and Soker (2006)].

Under what conditions is $r_{\text{sonic}} > r_{\text{tr}}$? One factor that can cause r_{sonic} to exceed r_{tr} is a small central black hole mass, since a smaller M_{bh} reduces r_{tr} . In addition, as illustrated in Quataert & Narayan’s approximate analytic results, if the black hole’s contribution to gravity were hypothetically ignored, r_{sonic} would increase with increasing \dot{M} . Thus, a sufficiently large \dot{M} can also cause r_{sonic} to exceed r_{tr} . A large \dot{M} results from either a large L_{cr} or a small accretion efficiency η . As discussed in the previous section, L_{cr} is approximately determined by the baryon density and temperature at the cooling radius - a higher density and/or lower temperature at r_{cool} means that thermal conduction can offset less of the radiative cooling within the cooling radius, which in turn leads to a larger L_{cr} . Thus, to summarize, smaller values of M_{bh} , η , or $T(r_{\text{cool}})$ and/or larger values of $\rho(r_{\text{cool}})$ can cause r_{sonic} to exceed r_{tr} , preventing a smooth transition from a cooling flow to an inner Bondi flow, and causing the cooling of intracluster plasma to low temperatures at $r > r_{\text{tr}}$.

We note that if the accretion efficiency η_{cool} that arises when plasma cools to low temperature outside r_{tr} is much smaller than the accretion efficiency η associated with Bondi accretion, then a flow that cools rapidly outside r_{tr} will need a much higher \dot{M} (and larger r_{cf}) in order for AGN feedback to provide the heating needed to offset cooling within the cooling radius. A much larger \dot{M} , in conjunction with plasma cooling to low temperatures outside r_{tr} , would imply a much larger star formation rate within the BCG. Thus, a small M_{bh} or large L_{cr} could lead to the condition $r_{\text{sonic}} > r_{\text{tr}}$ and cause star formation at rates that significantly exceed the Bondi accretion rates listed in table 3.

Returning to our model calculations, we list in table 3 the values of $|\langle v_r \rangle|/c_s$ at $r = r_1$ for the clusters in our sample. The value of $|\langle v_r \rangle|/c_s$ reaches its maximum at $r = r_1$ in our solutions, and

thus our solutions satisfy $|\langle v_r \rangle|/c_s < 1$ at all radii. Our calculations are thus at least marginally consistent with our assumptions of hydrostatic equilibrium and Bondi accretion. We also note that the sound crossing time t_s is shorter than cooling time t_{cool} at all radii in our model solutions. However, our model imposes an abrupt and artificial transition in the flow at $r = 0.2$ kpc, which causes our solution near $r = 0.2$ kpc to be inaccurate. In addition, there is significant uncertainty in the values of M_{bh} and η . It is thus possible that some of the clusters reach a sonic transition outside r_{tr} . Further investigation of this issue is needed.

6. Summary

There is a growing consensus that AGN feedback holds the key to solving the cooling-flow and overcooling problems for clusters of galaxies. However, the way in which an AGN’s power is delivered to the diffuse intracluster plasma is still not well understood. In this paper, we suggest that an AGN’s mechanical luminosity heats the intracluster plasma by accelerating cosmic rays that cause the intracluster medium to become convectively unstable. We explore this idea by developing a steady-state, mixing-length-theory model. By adjusting a single parameter in the model (the size of the cosmic-ray acceleration region, r_{source}), we obtain a good match to the observed density and temperature profiles in seven out of the eight clusters in our sample. Our model underestimates the density in the eighth cluster, Sersic 159-03, within the central ~ 50 kpc. We suggest that this discrepancy may result from the fact that the parameters in our NFW mass model are determined neglecting the cosmic-ray pressure. At the same time, Sersic 159-03 has the largest soft x-ray excess of any cluster observed by XMM, and likely contains a large population of non-thermal particles concentrated in the cluster core. (Werner 2007) If the mass model were recalculated taking the non-thermal pressure into account, the gravitational acceleration would be larger, especially in the cluster core, which would increase the plasma density at $r \lesssim 50$ kpc in our model calculations and possibly bring the model into agreement with the observations. We also find that the cosmic-ray luminosities of the AGN in our sample are strongly correlated with the observationally inferred mechanical luminosities of these AGN. Our results suggest that AGN-driven convection is an important process in cluster cores.

In our model solutions, the radiative cooling rate is much more peaked about $r = 0$ than is the rate of convective heating. As a result, a compact central cooling flow arises in our model calculations for several of the clusters in our sample. The radii, r_{cf} , of the cooling flows are typically a few kpc. The mass accretion rate onto the central AGN in these clusters is roughly the plasma mass at $r < r_{\text{cf}}$ divided by the cooling time at r_{cf} . We suggest that the AGN regulates the mass accretion rate in these clusters by controlling r_{cf} : if the AGN power rises above the equilibrium level, the size of the central cooling flow decreases, the mass accretion rate drops, and

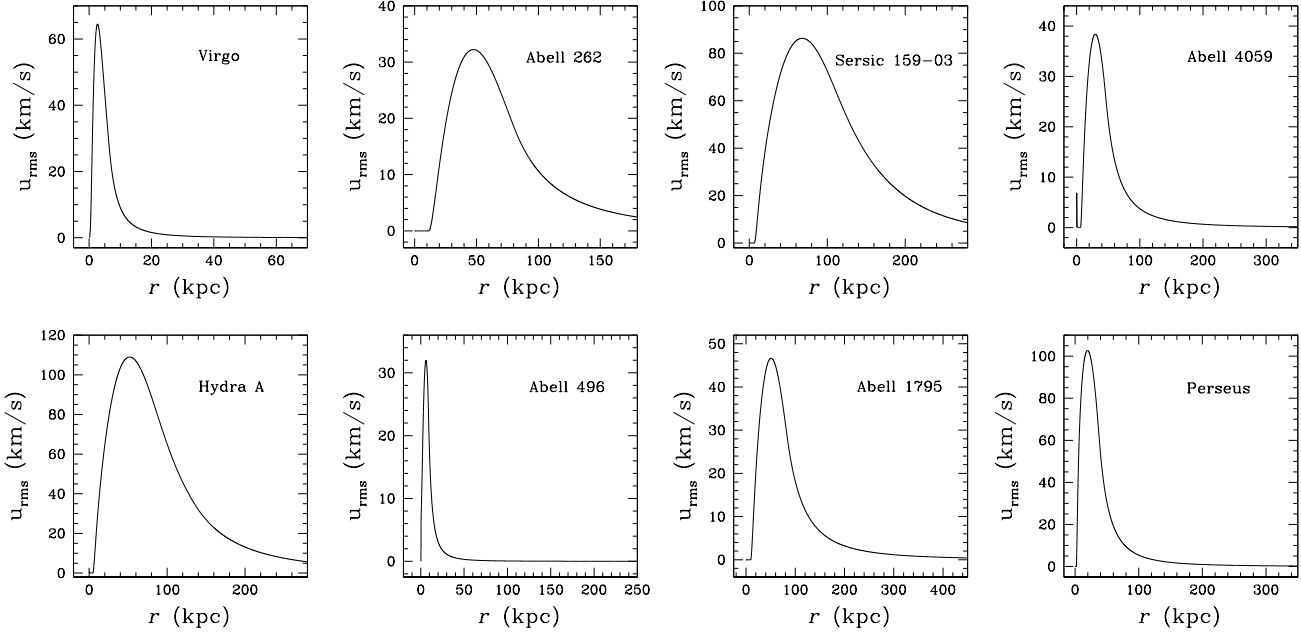


Fig. 5.— The rms turbulent velocity as a function of radius in the model solutions.

the AGN power then drops back down to the equilibrium level.

We thank Eric Blackman, Nadia Zakamska, Jelle Kaastra, and Eliot Quataert for helpful discussions. We acknowledge the usage of the HyperLeda database (<http://leda.univ-lyon1.fr>). This work was partially supported by NASA’s Astrophysical Theory Program under grant NNG 05GH39G and by NSF under grant AST 05-49577.

A. The profiles of the cosmic-ray pressure and turbulent velocity

The profiles of the rms turbulent velocity u_{rms} [defined in equation (B71)] and the cosmic-ray pressure (as a fraction of the thermal pressure) are plotted in figures 5 and 6. Although it is difficult to see in the cases of Sersic 159-03, Hydra A, Abell 496, and Abell 1795, figure 6 shows that $(d/dr)(p_{\text{cr}}/p) > 0$ at small r . [This can also be seen by comparing the figures with the values of $p_{\text{cr}}(r_1)/p(r_1)$ listed in table 3.] This is not because $dp_{\text{cr}}/dr > 0$ (in fact, $dp_{\text{cr}}/dr < 0$ at all r for each cluster), but instead because the thermal pressure decreases with radius more rapidly than the cosmic-ray pressure. We note that there was an error in one of the plotting subroutines used for paper II, which resulted in the velocities plotted in figure 4 of paper II being too large by a factor of 3.

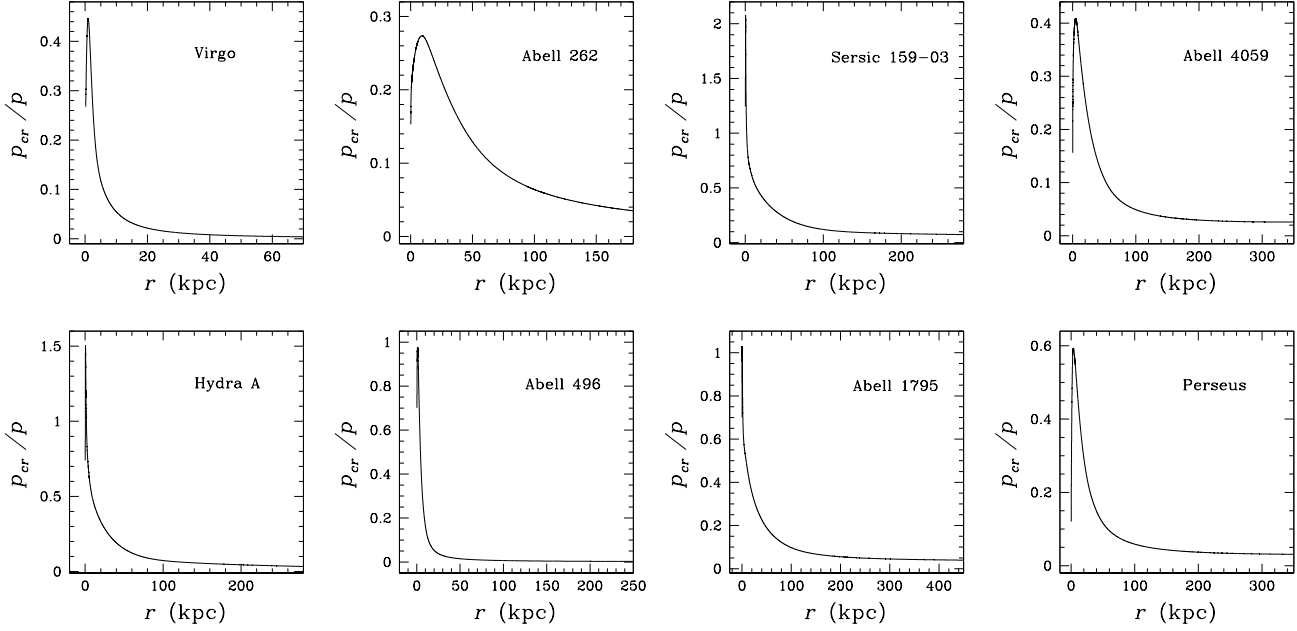


Fig. 6.— The ratio of cosmic-ray pressure to thermal pressure in the model solutions.

B. The two-fluid mixing-length theory and numerical method

In this appendix we describe the two-fluid mixing length theory that we use to model the convective intracluster medium. We take all fluid quantities to be the sum of an average value and a turbulent fluctuation, so that

$$\rho = \langle \rho \rangle + \delta \rho, \quad (\text{B1})$$

$$v = \langle v \rangle + \delta v, \quad (\text{B2})$$

etc. We take all average quantities to depend only on the radial coordinate r , and we set $\langle v \rangle = \langle v_r \rangle \hat{r}$. We wish to solve for four quantities: $\langle \rho \rangle$, $\langle v_r \rangle$, $\langle T \rangle$, and $\langle p_{\text{cr}} \rangle$. To do so we take the averages of four equations: equations (2), (3), and (5), as well as the total-energy equation. The latter is obtained by taking the dot product of equation (3) with v and adding the resulting equation to the sum of equations (4) and (5), which yields:

$$\begin{aligned} & \frac{\partial}{\partial t} \left(\frac{\rho v^2}{2} + \rho \Phi + \frac{p}{\gamma - 1} + \frac{p_{\text{cr}}}{\gamma_{\text{cr}} - 1} \right) \\ & + \nabla \cdot \left(\frac{\rho v v^2}{2} + \rho v \Phi + \frac{\gamma p v}{\gamma - 1} + \frac{\gamma_{\text{cr}} v p_{\text{cr}}}{\gamma_{\text{cr}} - 1} + \Gamma_{\text{visc}} - \kappa \cdot \nabla T - \frac{\mathbf{D} \cdot \nabla p_{\text{cr}}}{\gamma_{\text{cr}} - 1} \right) \\ & = \rho \frac{\partial \Phi}{\partial t} - R + \dot{E}_{\text{source}}, \end{aligned} \quad (\text{B3})$$

where Γ_{visc} is the viscous energy flux, and where we have made use of the relation $H_{\text{visc}} = (\nabla \cdot \Pi_{\text{visc}}) \cdot v = -\nabla \cdot \Gamma_{\text{visc}}$.⁴ We assume that the viscous energy flux is much less than the advective energy flux and thus drop Γ_{visc} . We also set $\partial\Phi/\partial t = 0$.

The average of equation (2) can be written

$$\langle v_r \rangle = -\frac{1}{\langle \rho \rangle} \left(Q + \frac{\dot{M}}{4\pi r^2} \right), \quad (\text{B4})$$

where

$$Q \equiv \langle \delta\rho\delta v_r \rangle, \quad (\text{B5})$$

and the mass accretion rate $\dot{M} = -4\pi r^2 \langle \rho v_r \rangle$ is a constant. The average of equation (3) yields

$$\frac{d}{dr} \langle p_{\text{tot}} \rangle = -\langle \rho \rangle \frac{d\Phi}{dr}, \quad (\text{B6})$$

where

$$p_{\text{tot}} = p + p_{\text{cr}} \quad (\text{B7})$$

is the total pressure. In writing equation (B6), we have taken the convection to be subsonic, so that the Reynolds stress can be neglected. We have also dropped the viscous stress, which is unimportant in the averaged equation. The average of equation (5) can be written

$$\begin{aligned} D_{\text{cr}} \frac{d^2 \langle p_{\text{cr}} \rangle}{dr^2} &= \frac{(1-\gamma)}{r^2} \frac{d}{dr} (r^2 F) + (1-\gamma_{\text{cr}}) (W + \langle \dot{E}_{\text{source}} \rangle) - \frac{d \langle p_{\text{cr}} \rangle}{dr} \left[\frac{1}{r^2} \frac{d}{dr} (r^2 D_{\text{cr}}) \right] \\ &+ \frac{\gamma_{\text{cr}} \langle p_{\text{cr}} \rangle}{r^2} \frac{d}{dr} (r^2 \langle v_r \rangle) + \langle v_r \rangle \frac{d \langle p_{\text{cr}} \rangle}{dr}, \end{aligned} \quad (\text{B8})$$

where

$$F \equiv \frac{\langle \delta v_r \delta p \rangle}{\gamma - 1}, \quad (\text{B9})$$

and

$$W \equiv \langle \delta p \nabla \cdot \delta v \rangle. \quad (\text{B10})$$

In writing equation (B8), we have again made use of the fact that the convection is subsonic, which implies that the total-pressure fluctuation is very small. As a result, we can set $\delta p \simeq -\delta p_{\text{cr}}$, $\langle \delta v_r \delta p_{\text{cr}} \rangle = -\langle \delta v_r \delta p \rangle$, and $\langle \delta p_{\text{cr}} \nabla \cdot \delta v \rangle = -\langle \delta p \nabla \cdot \delta v \rangle$. The average of equation (B3) yields

$$\kappa_T \frac{d^2 \langle T \rangle}{dr^2} = Q \frac{d\Phi}{dr} + \frac{\gamma p}{(\gamma-1)r^2} \frac{d}{dr} (r^2 \langle v_r \rangle) - \frac{\langle v_r \rangle}{\gamma-1} \left(\rho \frac{d\Phi}{dr} + \frac{dp_{\text{cr}}}{dr} \right) + \frac{1}{r^2} \frac{d}{dr} (r^2 F)$$

⁴The fact that the viscous terms can be written as a total divergence reflects the fact that viscosity is neither a source of energy nor a sink of energy, but instead merely converts bulk-flow energy into thermal energy. Thus, when equation (B3) is integrated over volume, Gauss's law can be used to express the viscous terms as a surface integral, which vanishes if the boundary of the integration lies outside the plasma.

$$+ W + R - \frac{d\langle T \rangle}{dr} \left[\frac{1}{r^2} \frac{d}{dr} (r^2 \kappa_T) \right], \quad (\text{B11})$$

where we have dropped the $\langle \rho v v^2 / 2 \rangle$ term since it is much smaller than the other terms for subsonic convection. In equation (B11), κ_T is the average (isotropic) thermal conductivity given by equations (24) and (25), where T is set equal to $\langle T \rangle$ in equation (24).

To solve equations (B4), (B6), (B8), and (B11) for $\langle \rho \rangle$, $\langle v_r \rangle$, $\langle T \rangle$, and $\langle p_{\text{cr}} \rangle$, we need to express the quantities Q , F , and W in terms of these average fluid quantities, thereby closing the equations. We accomplish this by using a two-fluid mixing length theory. Our approach is to first estimate Q , F , and W using a local mixing length theory. In the local theory, the properties of the turbulence at some radius are determined only by the average fluid properties and gradients at that radius. We then use this local theory as the basis for a non-local mixing length theory, as in paper II. In the nonlocal theory, the properties of the turbulence at some radius r are determined by a weighted average of the turbulence properties in the local mixing length theory over a range of radii. Our mixing-length theory differs from stellar mixing-length theory (Cox & Giuli 1968) in two important ways: we include a cosmic-ray fluid, and we take into account the fact that the diffusion of heat and cosmic rays occurs almost entirely along magnetic field lines.

We derive quantities in the local mixing length theory as follows. We take the convective turbulence to have a correlation length l , also called the mixing length, where

$$l = \alpha r, \quad (\text{B12})$$

α is a constant, and r is the distance from the center of the cluster. Fluid parcels in convective regions are taken to rise or sink a distance l before breaking up and mixing into the surrounding plasma. We take l to be much smaller than the pressure scale height, so that α is treated as $\ll 1$. (However, as in standard mixing-length theory, after the mixing-length-theory equations are derived, we relax the requirement that $\alpha \ll 1$, and set $\alpha = 0.4$ when applying the model to clusters in section 3.) We treat the fluctuations as small quantities, and take $\langle \sqrt{(\delta \rho)^2} \rangle / \langle \rho \rangle$, $\langle \sqrt{(\delta T)^2} \rangle / \langle T \rangle$, $\langle \sqrt{(\delta p_{\text{cr}})^2} \rangle / \langle p_{\text{cr}} \rangle$, and $\langle \sqrt{|\delta v|^2} \rangle / c_s$ to be $\sim O(\alpha)$ (meaning of order α), where c_s is the sound speed. We then expand the equations in powers of α , and keep only the lowest-order non-vanishing terms in this expansion. The quantities Q , F , and W involve products of fluctuating quantities, and are thus $\sim O(\alpha^2)$. We take R , $\langle \dot{E}_{\text{source}} \rangle$, κ_T , κ_{\parallel} , D_{cr} , D_{\parallel} , and H_{visc} to be $\sim O(\alpha^2)$, so that, e.g., radiative cooling, conduction, and turbulent heating are of the same order in α in equations (B8) and (B11). (Since the fluctuations are small, we can write, e.g., that $\langle p \rangle \simeq k_B \langle \rho \rangle \langle T \rangle / \mu m_H$, where μ is the mean molecular weight.) There are two contributions to the average velocity $\langle v \rangle$. One is driven by the turbulent fluctuations, and, as will be seen below, is of order α^2 . The second arises from the net inflow of mass towards the center of the cluster. In our model, the mass accretion rate is set by the Bondi accretion rate calculated from the plasma parameters at the inner

radius $r_1 = 0.2$ kpc, as described in section 2. We treat this second contribution to $\langle v \rangle$ as also of order α^2 .

We now proceed to estimate typical values for δT , $\delta \rho$, and δp_{cr} to first order in α - i.e., ignoring terms of order α^2 . Because we take the fluid displacement and the correlation length to be comparable, we need to use a Lagrangian approach to formally integrate the equations. We take the initial position of a fluid element at time $t = 0$ to be denoted r_0 , and its position at time t to be

$$r(r_0, t) = r_0 + \xi(r_0, t), \quad (\text{B13})$$

where ξ is the displacement of the fluid element. We use the shorthand notation that $\rho(t)$, $T(t)$, $p(t)$, $p_{\text{cr}}(t)$, and $\xi(t)$ are the density, temperature, pressure, cosmic-ray pressure, and displacement at time t of the fluid element that started at position r_0 at $t = 0$. The velocity at time t of the fluid element that starts at r_0 at $t = 0$ is given by

$$v = \left. \frac{\partial r}{\partial t} \right|_{r_0} = \left. \frac{\partial \xi}{\partial t} \right|_{r_0}. \quad (\text{B14})$$

We then have that

$$\left. \frac{\partial}{\partial t} \right|_{r_0} = \left. \frac{\partial}{\partial t} \right|_r + v \cdot \nabla, \quad (\text{B15})$$

where the spatial derivatives on the right-hand side are with respect to r , not r_0 . The Jacobian matrix \underline{J} for the transformation from r_0 to r is given by the equation

$$J_{ij} = \frac{\partial r_i}{\partial r_{0j}}. \quad (\text{B16})$$

The determinant of this matrix, denoted J , satisfies the equation

$$\left. \frac{\partial}{\partial t} \ln J \right|_{r_0} = \nabla \cdot v, \quad (\text{B17})$$

where the spatial derivatives on the right-hand side are again with respect to r , not r_0 .⁵ Using equations (B15) and (B17), we rewrite equation (2) as

$$\left. \frac{\partial \ln \rho}{\partial t} \right|_{r_0} = - \left. \frac{\partial \ln J}{\partial t} \right|_{r_0}. \quad (\text{B18})$$

⁵Equation B17 can be shown as follows. We define M_{ij} to be the determinant of the 2×2 matrix obtained by deleting the i^{th} row and j^{th} column of the matrix \underline{J} . We can then write that $\partial J / \partial J_{ij} = (-1)^{i+j} M_{ij}$. The inverse of \underline{J} , which we denote \underline{B} , satisfies $B_{ij} J_{jk} = \delta_{ik}$, and is given by $B_{ij} = (-1)^{i+j} M_{ji} / J$. We can thus write $\partial J / \partial t|_{r_0} = (\partial J / \partial J_{ij}) (\partial J_{ij} / \partial t)|_{r_0} = J B_{ji} (\partial J_{ij} / \partial t)|_{r_0}$. From the chain rule, $(\partial r_{0i} / \partial r_j) (\partial r_j / \partial r_{0k}) = \delta_{ik}$. Thus, $B_{ij} = \partial r_{0i} / \partial r_j$, and $(1/J) \partial J / \partial t|_{r_0} = (\partial r_{0j} / \partial r_i) [(\partial / \partial t)|_{r_0} (\partial r_i / \partial r_{0j})] = (\partial r_{0j} / \partial r_i) (\partial v_i / \partial r_{0j}) = \partial v_i / \partial r_i$.

We integrate equation (B18) in time from $t = 0$ to $t = \Delta t$ holding r_0 fixed (as in the time integrals below), where

$$\Delta t = \frac{l}{u_L} \quad (\text{B19})$$

is the “mixing time,” and u_L is the rms radial velocity in the local mixing length theory. We set $\xi(0) = 0$ and $\rho(0) = \langle \rho \rangle$, where $\langle \rho \rangle$ is shorthand notation for the average density at r_0 . We then obtain

$$\frac{\rho(\Delta t)}{\langle \rho \rangle} = \frac{1}{J(\Delta t)}, \quad (\text{B20})$$

where $J(\Delta t)$ is the Jacobian at $t = \Delta t$ evaluated for the initial position r_0 . If we start at $t = 0$ with a fluid element of infinitesimal volume $d^3 r_0$ centered at r_0 , then at time Δt its volume is $d^3 r = J(\Delta t) d^3 r_0$. Thus, equation (B20) is a statement of mass conservation. The Lagrangian density perturbation at time Δt is

$$\Delta \rho_{\text{Lag}} \equiv \rho(\Delta t) - \rho(0) = \rho(\Delta t) - \langle \rho \rangle. \quad (\text{B21})$$

Combining equations (B20) and (B21), we write

$$\frac{\Delta \rho_{\text{Lag}}}{\langle \rho \rangle} = \frac{1}{J(\Delta t)} - 1. \quad (\text{B22})$$

To solve for the pressure fluctuation, we write equation (4) in the form

$$\left. \frac{\partial p}{\partial t} \right|_{r_0} = -\gamma p \left. \frac{\partial \ln J}{\partial t} \right|_{r_0} + (\gamma - 1) \delta H_{\text{tc}}, \quad (\text{B23})$$

where

$$H_{\text{tc}} = \nabla \cdot (\kappa_{\parallel} \hat{b} \hat{b} \cdot \nabla T) \quad (\text{B24})$$

is the rate of heating due to thermal conduction, and δH_{tc} is the deviation of H_{tc} from its average value. In writing equation (B23), we have dropped terms of order α^2 . [$\delta H_{\text{tc}} \sim O(\alpha)$ since $\delta T \sim O(\alpha)$, $\kappa_{\parallel} \sim O(\alpha^2)$, and $\nabla^2 \delta T \sim \delta T / l^2 \sim O(\alpha^{-1})$.] We integrate equation (B23) from $t = 0$ to $t = \Delta t$, setting $\xi(0) = 0$ and $p(0) = \langle p \rangle$, where $\langle p \rangle$ is the average density at r_0 . To first order in α , we can replace $\gamma p \partial \ln J / \partial t|_{r_0}$ with $\gamma \langle p \rangle \partial \ln J / \partial t|_{r_0}$. We thus obtain

$$\Delta p_{\text{lag}} = -\gamma \langle p \rangle \ln J(\Delta t) + (\gamma - 1) \int_0^{\Delta t} \delta H_{\text{tc}}(t) dt, \quad (\text{B25})$$

where

$$\Delta p_{\text{Lag}} \equiv p(\Delta t) - p(0) = p(\Delta t) - \langle p \rangle, \quad (\text{B26})$$

is the Lagrangian pressure perturbation at time Δt . Because the density fluctuations are small, the value of $J(\Delta t)$ is very close to 1. Writing $J(\Delta t) = 1 + x$, the quantity x is of order α . Thus, $\ln J(\Delta t) = x + O(\alpha^2) = 1 - [J(\Delta t)]^{-1} + O(\alpha^2)$ and

$$\ln J(\Delta t) = -\frac{\Delta \rho_{\text{Lag}}}{\langle \rho \rangle} + O(\alpha^2). \quad (\text{B27})$$

To first order in α , we can thus rewrite equation (B25) as

$$\Delta p_{\text{lag}} = \frac{\gamma \langle p \rangle \Delta \rho_{\text{Lag}}}{\langle \rho \rangle} + (\gamma - 1) \int_0^{\Delta t} \delta H_{\text{tc}}(t) dt. \quad (\text{B28})$$

We have been analyzing a fluid element that starts off at $t = 0$ as an “average” fluid element, and we thus take $\delta T = 0$ and $\delta H_{\text{tc}} = 0$ at $t = 0$. When this fluid element is displaced radially outwards a distance l , it remains magnetically connected to the same set of fluid elements to which it was initially connected (at least until it is mixed into the surrounding fluid, at which point it is assumed that the magnetic field in the fluid parcel is randomized). This is depicted schematically in figure 7. If its temperature remains unchanged as it moves [i.e., if $\delta T_{\text{Lag}} \equiv T(t) - T(0) = 0$], then the effects of thermal conduction are unchanged and δH_{tc} will remain zero. However, if its temperature decreases, then more heat will be conducted into the fluid element, and δH_{tc} will increase. Thermal conduction will thus act to restore the temperature to its initial value (i.e. to keep $\delta T_{\text{Lag}} = 0$), with $\delta H_{\text{tc}} \propto -\delta T_{\text{Lag}}$ for small values of δT_{Lag} . To estimate δH_{tc} , we note that the mixing length l is comparable to the correlation lengths of both the convective turbulence and the temperature fluctuations. Thus, $|\nabla \delta T_{\text{Lag}}| \sim \delta T_{\text{Lag}}/l$, and we have the order-of-magnitude relation

$$\delta H_{\text{tc}} \sim -\frac{\kappa_{\parallel} \delta T_{\text{Lag}}}{l_T^2}. \quad (\text{B29})$$

We estimate that

$$(\gamma - 1) \int_0^{\Delta t} \delta H_{\text{tc}} dt = -\frac{0.3(\gamma - 1)\kappa_{\parallel} \Delta T_{\text{Lag}} \Delta t}{l^2}, \quad (\text{B30})$$

where $\Delta T_{\text{Lag}} = \delta T_{\text{Lag}}(\Delta t)$ is the Lagrangian temperature perturbation at time Δt , and the numerical factor of 0.3 is chosen somewhat arbitrarily to reflect (1) our expectation that the length scale of the temperature fluctuations is somewhat larger than l , which is just the radial component of the displacement vector, not the full modulus of ξ , and (2) the fact that δH_{tc} increases from zero to its maximum value as t ranges from 0 to Δt , so the typical value of δH_{tc} is less than its value at $t = \Delta t$. Finally, we obtain the relation

$$\Delta p_{\text{lag}} = \frac{\gamma \langle p \rangle \Delta \rho_{\text{Lag}}}{\langle \rho \rangle} - \frac{0.3(\gamma - 1)\kappa_{\parallel} \Delta T_{\text{Lag}} \Delta t}{l^2}. \quad (\text{B31})$$

To first order in α ,

$$\frac{\Delta T_{\text{Lag}}}{\langle T \rangle} = \frac{\Delta p_{\text{Lag}}}{\langle p \rangle} - \frac{\Delta \rho_{\text{Lag}}}{\langle \rho \rangle}, \quad (\text{B32})$$

where $\langle T \rangle$ is the average temperature at r_0 . Equations (B31) and (B32) combine to give

$$\Delta p_{\text{Lag}} = \Delta \rho_{\text{Lag}} \frac{\langle p \rangle}{\langle \rho \rangle} \left(\frac{\gamma + a_1}{1 + a_1} \right), \quad (\text{B33})$$

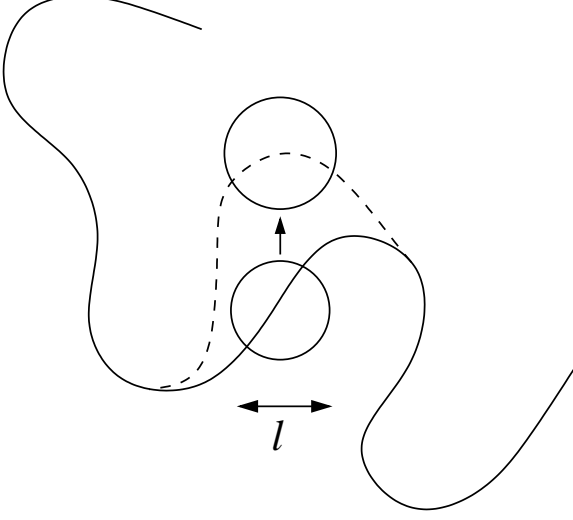


Fig. 7.— Schematic diagram of a rising fluid parcel. The solid line is a magnetic field line passing through the parcel’s initial location. The dashed line is an idealization of how the field line changes as a result of the fluid parcel’s displacement.

where

$$a_1 = \frac{0.3(\gamma - 1)\kappa_{\parallel}\langle T \rangle}{lu_{\text{L}}\langle p \rangle} \quad (\text{B34})$$

is roughly the ratio of the mixing time Δt to the time for heat to diffuse a distance l along the magnetic field. When $a_1 \ll 1$ the thermal plasma expands adiabatically, and when $a_1 \gg 1$ the thermal plasma expands isothermally.

To solve for the cosmic-ray pressure fluctuation, we write equation (5) in the form

$$\left. \frac{\partial p_{\text{cr}}}{\partial t} \right|_{r_0} = -\gamma_{\text{cr}} p_{\text{cr}} \left. \frac{\partial \ln J}{\partial t} \right|_{r_0} + \delta H_{\text{diff}} + (\gamma_{\text{cr}} - 1) \delta \dot{E}_{\text{source}}, \quad (\text{B35})$$

where

$$H_{\text{diff}} = \nabla \cdot (D_{\parallel} \hat{b} \hat{b} \cdot \nabla p_{\text{cr}}), \quad (\text{B36})$$

δH_{diff} is the deviation of H_{diff} from its average value, \dot{E}_{source} is the cosmic-ray energy per unit volume generated by the central radio source, and $\delta \dot{E}_{\text{source}}$ is the deviation of \dot{E}_{source} from its average value. As discussed in section 2.7, $\delta \dot{E}_{\text{source}}$ can be significantly larger than $\langle \dot{E}_{\text{source}} \rangle$ if the cosmic rays are accelerated in a small fraction of the volume. We thus treat $\delta \dot{E}_{\text{source}}$ as $O(\alpha)$ and $\langle \dot{E}_{\text{source}} \rangle$ as $O(\alpha^2)$. We integrate equation (B35) from $t = 0$ to $t = \Delta t$, setting $\xi(0) = 0$ and $p_{\text{cr}}(0) = \langle p_{\text{cr}} \rangle$, where $\langle p_{\text{cr}} \rangle$ is the average cosmic-ray pressure at r_0 . To first order in α , we can replace $\gamma_{\text{cr}} p_{\text{cr}} \partial \ln J / \partial t|_{r_0}$ with $\gamma_{\text{cr}} \langle p_{\text{cr}} \rangle \partial \ln J / \partial t|_{r_0}$. Using equation (B27), we obtain

$$\Delta p_{\text{cr,Lag}} = \frac{\gamma_{\text{cr}} \langle p_{\text{cr}} \rangle \Delta \rho_{\text{Lag}}}{\langle \rho \rangle} + \int_0^{\Delta t} [\delta H_{\text{diff}} + (\gamma_{\text{cr}} - 1) \delta \dot{E}_{\text{source}}] dt, \quad (\text{B37})$$

where

$$\Delta p_{\text{cr,Lag}} = p_{\text{cr}}(\Delta t) - \langle p_{\text{cr}} \rangle, \quad (\text{B38})$$

is the Lagrangian cosmic-ray pressure perturbation at time Δt .

We treat parallel cosmic-ray diffusion in the same way as parallel thermal conduction and make the estimate

$$\int_0^{\Delta t} \delta H_{\text{diff}} dt = -\frac{0.3D_{\parallel} \Delta p_{\text{cr,Lag}} \Delta t}{l^2}. \quad (\text{B39})$$

We assume that $\delta \dot{E}_{\text{source}}$ is typically positive in outwardly moving fluid elements and negative in inwardly moving fluid elements. Here, we are focusing on a fluid element that is moving outwards (the discussion can be repeated with little alteration for inwardly moving fluid parcels), and thus we treat $\delta \dot{E}_{\text{source}}$ as positive. We then make the estimate that

$$\int_0^{\Delta t} \delta \dot{E}_{\text{source}} dt = \delta \dot{E}_{\text{rms}} \Delta t, \quad (\text{B40})$$

where $\delta \dot{E}_{\text{rms}}$ is the rms value of $\delta \dot{E}_{\text{source}}$, which is determined from equation (35). Substituting (B39), and (B40) into equation (B37), we obtain

$$\Delta p_{\text{cr,Lag}} = \frac{\gamma_{\text{cr}} \langle p_{\text{cr}} \rangle \Delta p_{\text{Lag}}}{(1 + a_2) \langle \rho \rangle} + (\gamma_{\text{cr}} - 1) \delta \dot{E}_{\text{rms}} \tau, \quad (\text{B41})$$

where

$$\tau = \left(\frac{u_L}{l} + \frac{0.3D_{\parallel}}{l^2} \right)^{-1} \quad (\text{B42})$$

is the effective time during which cosmic rays can accumulate in the fluid parcel as a result of the cosmic-ray source term. (τ is roughly the shorter of the mixing time l/u_L and the diffusion time l^2/D_{\parallel} .) The quantity a_2 is given by

$$a_2 = \frac{0.3D_{\parallel}}{lu_L} \quad (\text{B43})$$

and is approximately the ratio of Δt to the time for cosmic rays to diffuse a distance l along the magnetic field. When $a_2 \ll 1$, the cosmic rays expand adiabatically if $\delta \dot{E}_{\text{rms}} = 0$. When $a_2 \gg 1$ the cosmic ray pressure in the fluid element remains constant as the element is displaced if $\delta \dot{E}_{\text{rms}} = 0$, as in the linear Parker instability in the large- D_{\parallel} limit (Parker 1966, Shu 1974, Ryu et al 2003).

Since it is assumed that the convection is subsonic, the total pressure in the fluid element remains approximately the same as the average total pressure in the fluid element's surroundings. We take

$$\hat{r} \cdot \xi(\Delta t) = l, \quad (\text{B44})$$

and thus to first order in α

$$\Delta p_{\text{Lag}} + \Delta p_{\text{cr,Lag}} = l \frac{d}{dr} \langle p_{\text{tot}} \rangle. \quad (\text{B45})$$

Adding equations (B33) and (B41) and using equation (B45), we obtain

$$l \frac{d}{dr} \langle p_{\text{tot}} \rangle = c_{\text{eff}}^2 \Delta \rho_{\text{Lag}} + (\gamma_{\text{cr}} - 1) \delta \dot{E}_{\text{rms}} \tau, \quad (\text{B46})$$

where

$$c_{\text{eff}} = \left[\left(\frac{\gamma + a_1}{1 + a_1} \right) \frac{\langle p \rangle}{\langle \rho \rangle} + \frac{\gamma_{\text{cr}} \langle p_{\text{cr}} \rangle}{(1 + a_2) \langle \rho \rangle} \right]^{1/2} \quad (\text{B47})$$

is an effective sound speed for the medium.

The fluctuating quantities appearing in equations (B5), (B9), and (B10) are Eulerian fluctuations, in that they involve the difference between some quantity and the average of that quantity at the same location. To first order in α , we can write the Eulerian density fluctuation of our outwardly displaced fluid element at time Δt , denoted $\Delta \rho$, as

$$\Delta \rho = \Delta \rho_{\text{Lag}} - l \frac{d\langle \rho \rangle}{dr}. \quad (\text{B48})$$

Combining equations (B46) and (B48), we find that

$$\Delta \rho = l \left(\frac{1}{c_{\text{eff}}^2} \frac{d\langle p_{\text{tot}} \rangle}{dr} - \frac{d\langle \rho \rangle}{dr} \right) - \frac{(\gamma_{\text{cr}} - 1) \delta \dot{E}_{\text{rms}} \tau}{c_{\text{eff}}^2}. \quad (\text{B49})$$

The fluid is convectively stable if an outwardly displaced parcel is heavier than its surroundings (i.e., if $\Delta \rho > 0$) for any value of u_L . We note that as u_L increases, a_1 and a_2 decrease, c_{eff}^2 increases, and τ decreases. Since $d\langle p_{\text{tot}} \rangle / dr < 0$, it follows that

$$\frac{d}{du_L} \Delta \rho > 0. \quad (\text{B50})$$

Thus, if $\Delta \rho > 0$ as $u_L \rightarrow 0$, then $\Delta \rho > 0$ for any u_L (u_L is by definition non-negative), and the medium is convectively stable. On the other hand, if $\Delta \rho < 0$ as $u_L \rightarrow 0$, then the medium is convectively unstable. The necessary and sufficient condition for convective stability is thus that $\Delta \rho$ be positive in the limit $u_L \rightarrow 0$. As $u_L \rightarrow 0$, we have that $a_1 \rightarrow \infty$, $a_2 \rightarrow \infty$, $\tau \rightarrow l^2 / (0.3 D_{\parallel})$, and $c_{\text{eff}}^2 \rightarrow \langle p \rangle / \langle \rho \rangle$. For constant mean molecular weight μ , this then leads to the stability criterion

$$l \left(nk_B \frac{dT}{dr} + \frac{dp_{\text{cr}}}{dr} \right) - \frac{(\gamma_{\text{cr}} - 1) \delta \dot{E}_{\text{rms}} l^2}{0.3 D_{\parallel}} > 0, \quad (\text{B51})$$

where $n = \rho / (\mu m_H)$ is the number density of thermal particles. If one sets $\delta \dot{E}_{\text{rms}}$ to zero, then equation (B51) reduces to the stability criterion derived by Chandran (2005) and Chandran & Dennis (2006). Here, we have kept the fluctuations in \dot{E}_{source} , which act to destabilize the medium to convection, since localized excesses in the cosmic-ray pressure lead to pockets of buoyant, lower-density fluid.

If the convective stability criterion is satisfied at some radius, we set the local convective velocity u_L to zero at that radius. Otherwise the fluid is convectively unstable, and we estimate the value of u_L by solving the polynomial equation

$$\frac{\langle \rho \rangle u_L^2}{2} = \left| \frac{l \Delta \rho}{16} \frac{d\Phi}{dr} \right|. \quad (\text{B52})$$

Equation (B52) states that the mean radial kinetic energy of the fluid element is the mixing length times the buoyancy force on the fully displaced parcel times the numerical factor of $1/16$ that is commonly used in one-fluid mixing length theory (Cox & Giuli 1968). Once u_L is found, we determine $\Delta \rho_{\text{Lag}}$ and Δp_{Lag} using equations (B46) and (B33), respectively. The Eulerian pressure perturbation at time Δt , denoted Δp , is then given by the equation

$$\Delta p = \Delta p_{\text{Lag}} - l \frac{d\langle p \rangle}{dr}. \quad (\text{B53})$$

We then estimate the quantity F in equation (B9) to be

$$F_L = \frac{c_{\text{avg}} u_L \Delta p}{\gamma - 1}. \quad (\text{B54})$$

Here, as below, the L subscript is used to denote the estimate obtained using local mixing length theory. We set

$$c_{\text{avg}} = 1/2 \quad (\text{B55})$$

to match standard treatments of local one-fluid mixing length theory (Cox & Giuli 1968). We estimate the quantity Q in equation (B5) to be

$$Q_L = c_{\text{avg}} u_L \Delta \rho, \quad (\text{B56})$$

with $\Delta \rho$ determined from equation (B49). We estimate the quantity W in equation (B10) by noting that $\int_0^{\Delta t} \nabla \cdot v dt = -\ln \left[\frac{\rho(\Delta t)}{\langle \rho \rangle} \right] = -\ln \left[1 + \frac{\Delta \rho_{\text{Lag}}}{\langle \rho \rangle} \right] \simeq -\frac{\Delta \rho_{\text{Lag}}}{\langle \rho \rangle}$. Thus, the typical value of $\nabla \cdot \delta v$ is $\frac{1}{\Delta t} \left(-\frac{\Delta \rho_{\text{Lag}}}{\langle \rho \rangle} \right) = -\frac{u \Delta \rho_{\text{Lag}}}{l \langle \rho \rangle}$. We thus set

$$W_L = -\frac{c_{\text{avg}} u_L \Delta p \Delta \rho_{\text{Lag}}}{l \langle \rho \rangle}. \quad (\text{B57})$$

Having estimated Q , F , and W using local mixing length theory, we now use these estimates as the basis for a nonlocal theory. In the study of Ulrich (1976), the nonlocal heat flux is given by a weighted spatial average of the heat flux obtained from local mixing length theory. We adopt the same approach and set

$$F_{\text{NL}}(z) = \int_{-\infty}^{\infty} dz_1 F_L(z_1) \Psi_F(z - z_1), \quad (\text{B58})$$

$$W_{\text{NL}}(z) = \int_{-\infty}^{\infty} dz_1 W_L(z_1) \psi_W(z - z_1), \quad (\text{B59})$$

and

$$Q_{\text{NL}}(z) = \int_{-\infty}^{\infty} dz_1 Q_L(z_1) \psi_Q(z - z_1), \quad (\text{B60})$$

where

$$z = \ln \left(\frac{r}{r_{\text{ref}}} \right), \quad (\text{B61})$$

r_{ref} is an unimportant constant, and the NL subscripts denote values in our nonlocal theory. Different forms for the kernel function ψ_F were considered by Ulrich (1976). Here, we adopt the following values:

$$\psi_Q(x) = \psi_F(x) = \begin{cases} \alpha^{-1} e^{-x/\alpha} & \text{if } x > 0 \\ 0 & \text{if } x \leq 0 \end{cases}, \quad (\text{B62})$$

and

$$\psi_W(x) = \begin{cases} \alpha_W^{-1} e^{-x/\alpha_W} & \text{if } x > 0 \\ 0 & \text{if } x \leq 0 \end{cases}. \quad (\text{B63})$$

Equations (B58) through (B63) are equivalent to the differential equations

$$\alpha r \frac{dF_{\text{NL}}}{dr} + F_{\text{NL}} = F_L, \quad (\text{B64})$$

$$\alpha r \frac{dQ_{\text{NL}}}{dr} + Q_{\text{NL}} = Q_L, \quad (\text{B65})$$

and

$$\alpha_W r \frac{dW_{\text{NL}}}{dr} + W_{\text{NL}} = W_L. \quad (\text{B66})$$

For $r > r_{\text{conv}}$, where r_{conv} is the largest radius at which the fluid is locally unstable to convection, $F_L = 0$ and $F_{\text{NL}} \propto r^{-1/\alpha}$. When F and W are set equal to F_{NL} and W_{NL} in equations (B8) and (B11), the terms containing F_{NL} are $\propto r^{-1-1/\alpha}$ for $r > r_{\text{conv}}$. To obtain the same scaling for the terms containing W_{NL} , the value of α_W is determined from the equation

$$\alpha_W^{-1} = \alpha^{-1} + 1. \quad (\text{B67})$$

Equations (B62) and (B63) represent a one-sided average, in the sense that the nonlocal quantities F_{NL} , Q_{NL} , and W_{NL} depend only on the values of F_L , Q_L , and W_L at smaller radii. A more sophisticated nonlocal theory could be developed along different lines (see e.g. Travis & Matsushima 1973, Ulrich 1976, Xiong 1991, Grossman, Narayan, & Arnett 1993), but is beyond the scope of this paper.

The final equations for our mixing-length model are then equations (B4), (B6), (B8), (B11), (B64), (B65), and (B66), which form a system of two second-order ordinary differential equations

(ODEs), four first-order ODEs, and one algebraic equation [equation (B4)] for the seven variables $\langle \rho \rangle$, $\langle v_r \rangle$, $\langle T \rangle$, $\langle p_{\text{cr}} \rangle$, F_{NL} , Q_{NL} , and W_{NL} . Eight boundary conditions are required to specify a solution. Two boundary conditions are obtained by requiring that the model density and temperature match the observed values ρ_{outer} and T_{outer} at the outer radius r_{outer} . For seven of the eight clusters in our sample (all except Virgo), we choose r_{outer} to be the center of the first radial bin outside the cooling radius r_{cool} . Values of r_{cool} for each cluster are given in table 2. For Virgo, we take r_{outer} to be the outermost data point, which lies inside of r_{cool} . Since we do not solve all the way in to the sonic point, we are forced to pick inner boundary conditions (at $r_1 = 0.2$ kpc) in a somewhat arbitrary way. We take $d\langle T \rangle/dr$, $d\langle p_{\text{cr}} \rangle/dr$, F_{NL} , W_{NL} , and Q_{NL} to vanish at $r = r_1$. These “no-flux” boundary conditions set the diffusive and turbulent energy fluxes to zero at the inner boundary. Although this choice is undoubtedly inaccurate, we expect that it has only a small effect on our solution for the structure of the intracluster medium at $r \gg r_1$. The eighth boundary condition is obtained by assuming that $\langle p_{\text{cr}} \rangle \rightarrow 0$ as $r \rightarrow \infty$. This condition is translated into a condition on $\langle p_{\text{cr}} \rangle$ at r_{outer} as follows. The value of r_{outer} is chosen to be significantly greater than r_{source} and much greater than D_0/v_d , so that for $r > r_{\text{outer}}$, \dot{E}_{source} is negligible and $D_{\text{cr}} \simeq v_d r$.⁶ In addition, r_{outer} is taken to lie outside r_{conv} , the largest radius at which the intracluster medium is locally convectively unstable, so that $F_{\text{NL}} = F_{\text{outer}}(r/r_{\text{outer}})^{-1/\alpha}$ and $W_{\text{NL}} = W_{\text{outer}}(r/r_{\text{outer}})^{-1-1/\alpha}$ for $r > r_{\text{outer}}$, where F_{outer} and W_{outer} are the values of F_{NL} and W_{NL} at $r = r_{\text{outer}}$. We also take $\langle v_r \rangle$ to be negligible for $r > r_{\text{outer}}$. This latter assumption is reasonable, since $Q_{\text{NL}} = Q_{\text{outer}}(r/r_{\text{outer}})^{-1/\alpha}$ for $r > r_{\text{conv}}$, where Q_{outer} is the value of Q_{NL} at r_{outer} . The resulting value of $\langle v_r \rangle$ is significantly less than v_d for $r > r_{\text{conv}}$ in the numerical solutions we present in section 3, and thus $\langle v_r \rangle$ plays only a small role in equation (B8) at $r > r_{\text{conv}}$. Solving equation (B8) and requiring that $\langle p_{\text{cr}} \rangle \rightarrow 0$ as $r \rightarrow \infty$, we find that for $r \geq r_{\text{outer}}$

$$\frac{d\langle p_{\text{cr}} \rangle}{dr} = \frac{\chi}{v_d r^{1+1/\alpha}} - \frac{2\langle p_{\text{cr}} \rangle}{r}, \quad (\text{B68})$$

where

$$\chi = (2\alpha - 1)(\gamma - 1)F_{\text{outer}}r_{\text{outer}}^{1/\alpha} + \alpha(\gamma_{\text{cr}} - 1)W_{\text{outer}}r_{\text{outer}}^{1+1/\alpha}. \quad (\text{B69})$$

Equation (B68) applied at $r = r_{\text{outer}}$ provides the eighth boundary condition. We then solve our system of equations using a shooting method. We guess the values of $\langle \rho \rangle$, $\langle T \rangle$, and $\langle p_{\text{cr}} \rangle$ at $r = r_1$ and then integrate the equations from $r = r_1$ to $r = r_{\text{outer}}$. We then update our three guesses using Newton’s method until the three boundary conditions at r_{outer} are met.

To compare to future observations and to analyze the turbulent diffusion of metals in the ICM [see, e.g., Rebusco et al (2005)], it is of interest to calculate the rms turbulent velocity. We define

⁶The case $v_d = 0$ requires a different approach and is not treated in this paper.

a nonlocal turbulent velocity, u_{NL} , through the equation

$$\alpha r \frac{du_{\text{NL}}}{dr} + u_{\text{NL}} = u_L. \quad (\text{B70})$$

Since u_L (and thus u_{NL}) is an estimate of the radial component of the velocity of a convective fluid element, the full rms turbulent velocity is roughly

$$u_{\text{rms}} = \sqrt{3} u_{\text{NL}}, \quad (\text{B71})$$

which is the quantity plotted in figure 5.

REFERENCES

- Allen, S. W., Dunn, R. J. H., Fabian, A. C., Taylor, G. B., Reynolds, C. S. 2006, MNRAS, 372, 21
- Balbus, S. 2000, ApJ, 534, 420
- Balbus, S. 2001, ApJ, 562, 909
- Begelman, M. C. 2001, in ASP Conf. Proc., 240, *Gas and Galaxy Evolution*, ed. J. E. Hibbard, M. P. Rupen, & J. H. van Gorkom (San Fransisco: ASP), 363
- Begelman, M. C. 2002, in ASP Conf. Proc., 250, *Particles and Fields in Radio Galaxies*, ed. R. A. Laing, & K. M. Blundell (San Fransisco: ASP), 443
- Bieber, J. Matthaeus, W., Smith, C., Wanner, W., Kallenrode, M., & Wibberenz, G. 1994, ApJ, 420, 294
- Binney, J., & Tabor, G. 1995, MNRAS, 276, 663
- Birzan, L., Rafferty, D., McNamara, B., Wise, M., & Nulsen, P. 2004, ApJ, 607, 800
- Blanton, E., Sarazin, C., & McNamara, B. 2003, ApJ, 585, 227
- Böhringer, H. et al 2001, A&A, 365, L181
- Böhringer, H., & Morfill, G. 1988, ApJ, 330, 609
- Böhringer, H., Matsushita, K., Churazov, E., & Finoguenov, A. 2004a, in *The Riddle of Cooling Flows and Clusters of Galaxies*, ed. Reiprich, T., Kempner, J., & Soker, N., E3, <http://www.astro.virginia.edu/coolflow/proc.php>
- Bondi, H. 1952, MNRAS, 112, 159
- Braginskii, S. I. 1965, in *Reviews of Plasma Physics*, vol. 1, ed. M. A. Leontovich (New York: Consultants Bureau), 205
- Cattaneo, A., & Teyssier, R. 2007, MNRAS, 192

- Chandran, B. 2000a, Phys. Rev. Lett., 85, 4656
- Chandran, B. 2004, ApJ, 616, 169 (Paper I)
- Chandran, B. 2005, ApJ, 632, 809 (Paper II)
- Chandran, B., & Cowley, S. 1998, Phys. Rev. Lett., 80, 3077
- Chandran, B., & Dennis, T. 2006, ApJ, 642, 140
- Chandran, B., Maron, J. 2004, ApJ, 602, 170
- Churazov, E., Brüggén, M., Kaiser, C., Böhringer, H., & Forman, W. 2001, ApJ, 554, 261
- Churazov, E., Forman, W., Jones, C., Sunyaev, R., & Böhringer, H. 2004, MNRAS, 347, 29
- Churazov, E., Sunyaev, R., Forman, W., & Böhringer, H. 2002, MNRAS, 332, 729
- Ciotti, L., & Ostriker, J. 1997, ApJ, 487, L105
- Ciotti, L., & Ostriker, J. 2001, ApJ, 551, 131
- Ciotti, L., & Ostriker, J., & Pellegrini, S. 2004, in *Plasmas in the Laboratory and in the Universe: New Insights and New Challenges*,
- Cox, D. P. 2000, Allen’s Astrophysical Quantities (New York: AIP)
- David, L. P., Nulsen, P. E. J., McNamara, B. R., Forman, W., Jones, C., Ponman, T., Robertson, B., Wise, M. 2001, ApJ, 557, 546
- Dennis, T., & Chandran, B. 2005, 622, 205
- Di Matteo, T., Allen, S. W., Fabian, A. C., Wilson, A. S., & Young, A. J. 2003, ApJ, 582, 133
- Drury, L., & Volk, H. 1981, ApJ, 248, 344
- Eilek, J. 2004, in *The Riddle of Cooling Flows and Clusters of Galaxies*, ed. Reiprich, T., Kempner, J., & Soker, N., E13, <http://www.astro.virginia.edu/coolflow/proc.php>
- Fabian, A. C. 1994, Ann. Rev. Astr. Astrophys., 32, 277
- Fabian, A. C., Sanders, J., Allen, S., Crawford, C., Iwasawa, K., Johnstone, M., Schmidt, R., & Taylor, G. 2003, MNRAS, 344, L43
- Fabian, A. C. 1994, Ann. Rev. Astr. Astrophys., 32, 277
- Goldreich, P. & Sridhar, S. 1995, ApJ, 438, 763
- Graham, A., Merritt, D., Moore, B., Diemand, J., & Terzić, B. 2006, ApJ, 132, 2711
- Graham, A., Lauer, T. R., Colless, M., & Postman, M. 1996, ApJ, 465, 534
- Grossman, S., Narayan, R., & Arnett, D. 1993, ApJ, 407, 284
- Hernquist, L. 1990, ApJ, 356, 359

- Hoefl, M., & Brüggen, M. 2004, ApJ, 617, 896
- Kaastra, J. S., Tamura, T., Peterson, J., Bleeker, J., Ferrigno, C., Kahn, S., Paerels, F., Piffaretti, R., Branduardi-Raymont, G., & Böhringer, H. 2004, A&A, 413, 415
- Kronberg, P. 1994, Rep. Prog. Phys., 57, 325
- Jones, T., & Kang, H. 1990, ApJ, 363, 499
- Kim, W., & Narayan, R. 2003, ApJ, 596, L139
- Lauer, T. R., Faber, S. M., Richstone, D., Gebhardt, K., Tremaine, S., Postman, M., Dressler, A., Aller, M. C., Filippenko, A. V., Green, R., Ho, L. C., Kormendy, J., Magorrian, J., Pinkney, J. 2007, ApJ, 662, 808
- Lazarian, A. 2006, ApJL, 645, 25
- Lewis, G. F., Babul, A., Katz, N., Quinn, T., Hernquist, L., & Weinberg, D. 2000, ApJ, 536, 623
- Loewenstein, M., & Fabian, A. 1990, MNRAS, 242 120
- Loewenstein, M., Zweibel, E., & Begelman, M. 1991, ApJ, 377, 392
- Maron, J., Chandran, B., & Blackman, E. 2004, Phys. Rev. Lett., 92, id. 045001
- McLaughlin, D. 1999, ApJ, 512, L9
- Molendi, S., & Pizzolatto, F. 2001, ApJ, 560, 194
- Nagai, D., & Kravtsov, A. 2004, in IAU Colloq. 195, Outskirts of Galaxy Clusters: Intense Life in the Suburbs, ed. A. Diaferio (Cambridge: Cambridge Univ. Press), 296
- Narayan, R., & Medvedev, M. 2001, ApJ, 562, 129
- Navarro, J., Frenk, C., & White, S. 1997, ApJ, 490, 493
- Nulsen, P. 2004, in *The Riddle of Cooling Flows and Clusters of Galaxies*, ed. Reiprich, T., Kempner, J., & Soker, N., E30, <http://www.astro.virginia.edu/coolflow/proc.php>
- Owen, F., & Ledlow, M. 1997, ApJS, 108, 410
- Parrish, I., & Stone, J., 2005, ApJ, 633, 334
- Parrish, I., & Stone, J. 2006, astro-ph/0612195
- Paturel, G.; Petit, C.; Prugniel, Ph.; Theureau, G.; Rousseau, J.; Brouty, M.; Dubois, P.; Cambrsy, L. 2003, A&A, 412, 45-55
- Peterson, J. R., et al 2001, A&A, 365, L104
- Peterson, J. R., Kahn, S., Paerels, F., Kaastra, J., Tamura, T., Bleeker, J., Ferrigno, C., & Jernigan, J. 2003, ApJ, 590, 207
- Piffaretti, R., Jetzer, Ph., Kaastra, J., Tamura, T. 2005, A&A, 433, 101

- Piffaretti, R., & Kaastra, J. 2006, *A&A*, 453, 423
- Pizzolato, F., & Soker, N. 2005, *ApJ*, 632, 821
- Quataert, E. 1998, *ApJ*, 500, 978
- Quataert, E., & Narayan, R. 2000, *ApJ*, 528, 236
- Rasera, Y., & Chandran, B. 2007, *ApJ*, submitted
- Rebusco, P., Churazov, E., Bhringer, H., Forman, W. 2005, *MNRAS*, 359, 1041
- Rechester, R., & Rosenbluth, M. 1978, *Phys. Rev. Lett.*, 40, 38
- Reynolds, C. S. 2002, in *ASP Conf. Proc.*, 250, *Particles and Fields in Radio Galaxies*, ed. R. A. Laing, & K. M. Blundell (San Fransisco: ASP), 449
- Reynolds, C. S., McKernan, B., Fabian, A., Stone, J., & Vernaleo, J. 2005, *MNRAS*
- Rosner, R., & Tucker, W. 1989, *ApJ*, 338 761
- Ruszkowski, M., & Begelman, M. 2002, 581, 223
- Ruszkowski, M., Bruggen, M., & Begelman, M. 2004a, *ApJ*, 611, 158
- Ruszkowski, M., Bruggen, M., & Begelman, M. 2004b, *ApJ*, 615, 675
- Sazonov, S. Y., Ostriker, J. P., Ciotti, L., & Sunyaev, R. A. 2005, *MNRAS*, 358, 168
- Schekochihin, A. A., Cowley, S. C., Kulsrud, R. M., Hammett, G. W., & Sharma, P. 2006, *ApJ*, 629, 139
- Schekochihin, A. A. & Cowley, S. C. 2006, *Phys. Plasmas*, 13, 056501
- Schombert, J. M. 1987, *APJS*, 64, 643
- Soker, N. 2006, *New Astronomy*, 12, 38
- Spitzer, L., & Harm, R. 1953, *Phys. Rev.*, 89, 977
- Springel, V., Di Matteo, T., & Hernquist, L. 2005, *MNRAS*, 361, 776
- Suginohara, T., & Ostriker, J. 1998, *ApJ*, 507, 16
- Tabor, G., & Binney, J. 1993, *MNRAS*, 263, 323
- Tan, J., & Blackman, E. 2005, *MNRAS*, 362, 983
- Taylor, G., Fabian, A., Allen, S. 2002, *MNRAS*, 334, 769
- Taylor, G., Govoni, F., Allen, S., Fabian, A. 2001, *MNRAS*, 326, 2
- Tamura, T. et al 2001, *A&A*, 365, L87
- Tornatore, L., Borgani, S., Springel, V., Matteucci, F., Menci, N., & Murante, G. 2003, *MNRAS*, 342, 1025

- Tozzi, P., & Norman, C. 2001, *ApJ*, 546, 63
- Travis, L., & Matsushima, S. 1973, *ApJ*, 180, 975
- Ulrich, R. 1976, *ApJ*, 207, 564
- Vogt, C., & Ensslin, T. 2003, *A&A*, 412, 373
- Vogt, C., & Ensslin, T. 2005, *A&A*, 434, 67
- Voigt, L., & Fabian, A. 2004, *MNRAS*, 347, 1130
- Werner, N., Kaastra, J. S., Takei, Y., Lieu, R., Vink, J., & Tamura, T. 2007, *A&A*, 468, 849
- Worthey, G. 1994, *ApJ*, 95, 107
- Xiong, D. R. 1991, *Proc. Astr. Soc. Australia*, 9, 26
- Yan, H., & Lazarian, A. 2004, *ApJ*, 614, 757
- Zakamska, N., & Narayan, R. 2003, *ApJ*, 582, 162